

## Stabilization of p53 by microRNAs in HPV-positive cervical cancer cells

— [Source link](#) 

Gustavo Martínez-Noël, Patricia Szajner, Jennifer A. Smith, Kathleen A. Boyland ...+2 more authors

**Institutions:** Harvard University

**Published on:** 21 Sep 2020 - bioRxiv (Cold Spring Harbor Laboratory)

**Topics:** Cancer cell, Cancer, Ubiquitin ligase, HeLa and microRNA

Related papers:

- [Interferon- \$\beta\$  induced microRNA-129-5p down-regulates HPV-18 E6 and E7 viral gene expression by targeting SP1 in cervical cancer cells.](#)
- [Human Papillomavirus E6/E7 and Long Noncoding RNA TMPOP2 Mutually Upregulated Gene Expression in Cervical Cancer Cells.](#)
- [Proteomics Analysis of Andrographolide-Induced Apoptosis via the Regulation of Tumor Suppressor p53 Proteolysis in Cervical Cancer-Derived Human Papillomavirus 16-Positive Cell Lines.](#)
- [Oncogenic viral protein HPV E7 up-regulates the SIRT1 longevity protein in human cervical cancer cells](#)
- [Human papillomavirus 16 E2 regulates keratinocyte gene expression relevant to cancer and the viral life cycle](#)

Share this paper:    

View more about this paper here: <https://typeset.io/papers/stabilization-of-p53-by-micrnas-in-hpv-positive-cervical-4aynr283vx>

1 **Stabilization of p53 by microRNAs in HPV-positive**  
2 **cervical cancer cells**

3

4 Gustavo Martínez-Noël<sup>1,3</sup>, Patricia Szajner<sup>1,3</sup>, Jennifer A. Smith<sup>1,2</sup>, Kathleen Boyland<sup>1</sup>,  
5 Rebecca E. Kramer<sup>1</sup>, and Peter M. Howley<sup>1\*</sup>

6

7 <sup>1</sup>Department of Immunology, Harvard Medical School, 77 Avenue Louis

8 Pasteur, Boston MA 02115

9 <sup>2</sup>ICCB-Longwood Screening Facility, Harvard Medical School, 250 Longwood Avenue,

10 Boston MA 02115

11 <sup>3</sup>These authors contributed equally: Gustavo Martínez-Noël, Patricia Szajner

12

13

14 Abstract word count: 226

15 Text word count: 10,143

16

17

18 \*Corresponding author, Phone: 617-432-2889; Fax 617-432-2882

19 Email: Peter\_howley@hms.harvard.edu

20

21 Running Title: HPV p53 miRNA Stabilization Screen

## 22 **Abstract**

23 Etiologically 5% of cancers worldwide are caused by the high-risk human  
24 papillomaviruses (hrHPVs). These viruses encode two oncoproteins (E6 and E7)  
25 whose expression is required for cancer initiation and maintenance. Among the  
26 cellular targets of these viral oncoproteins are the p53 and the retinoblastoma  
27 tumor suppressor proteins. Inhibition of E6-mediated ubiquitylation of p53 through  
28 the E6AP ubiquitin ligase results in the stabilization of p53, leading to cellular  
29 apoptosis. We utilized a live cell high-throughput screen to assess the ability of 885  
30 microRNAs (miRNAs) to stabilize p53 in human papillomavirus (HPV)-positive  
31 cervical cancer cells expressing a p53-fluorescent protein as an *in vivo* reporter of  
32 p53 stability. The 32 miRNAs whose expression resulted in the greatest p53  
33 stabilization were further assessed in validation experiments using a second cell-  
34 based p53 stability reporter system as well as in HeLa cells to examine their effects  
35 on endogenous p53 protein levels. The positive miRNAs identified included 375-3p  
36 that has previously been reported as stabilizing p53 in HeLa cells, providing  
37 validation of the screen. Additional miRNAs that stabilized p53 led to decreases in  
38 E6AP protein levels, while others, including members of the 302/519 family of  
39 miRNAs, targeted HPV oncoprotein expression. We further examined a subset of  
40 these miRNAs for their abilities to induce apoptosis and determined whether the  
41 apoptosis was p53-mediated. The miRNAs described here have potential as  
42 therapeutics for treating HPV-positive cancers.

## 43 **Author summary**

44 Human papillomaviruses cause approximately 5% of cancers worldwide and encode genes  
45 that contribute to both the initiation and maintenance of these cancers. The viral gene E6 is  
46 expressed in all HPV-positive cancers and functions by targeting the degradation of the p53  
47 protein through its engagement of the cellular ubiquitin ligase E6AP. Inhibiting the  
48 degradation of p53 results in apoptosis in HPV-positive cancer cells. We have developed a  
49 high-throughput live cell assay to identify molecules that stabilize p53 in HPV-positive cells  
50 and we present the results of a screen we have carried out examining miRNAs for their  
51 abilities to stabilize p53 and induce apoptosis in HPV-positive cervical cancer cells. These  
52 miRNAs have the potential to be used in the treatment of HPV-positive cancers.

## 53 **Introduction**

54 Cervical cancer is the second leading cause of cancer deaths among women worldwide,  
55 with approximately 500,000 new cases diagnosed and 275,000 deaths each year. Virtually  
56 all cases of cervical cancer are attributable to infection by HPVs. There are over 200  
57 different HPV types and a subset of these are linked to anogenital tract infections, 14 of  
58 which are referred to as hrHPV because they are associated with lesions that can progress  
59 to cancer [1]. These same hrHPVs are also associated with other genital tract cancers  
60 (penile, vaginal, vulvar, and anal), as well as an increasing number of oropharyngeal  
61 cancers. Indeed, approximately 5% of cancers worldwide are caused by HPV [2].  
62 Despite the success of the virus like particle (VLP)-based vaccine that will prevent millions  
63 of new HPV-associated cancers, there is the need for effective therapies to treat cancers  
64 that will develop in individuals who have not been vaccinated and those already infected

65 with hrHPVs. In this regard, hrHPVs provide a number of potential viral targets for specific  
66 HPV antiviral therapies, including the viral encoded oncoproteins E6 and E7, the viral E1  
67 helicase, and the viral E2 regulatory protein.

68 The hrHPVs associated with cervical cancer encode two oncoproteins, E6 and E7, that are  
69 invariably expressed in HPV-positive cancers and target the important cellular growth  
70 regulatory proteins p53 and pRb, respectively [1]. These cancers are dependent upon the  
71 continued expression of E6 and E7 and silencing of E6 and E7 expression results in  
72 apoptosis and senescence [3, 4]. The E6 proteins of the hrHPV types promote the ubiquitin-  
73 dependent degradation of the p53 protein [5] through its binding interaction with the E3  
74 ubiquitin ligase E6AP (also known as UBE3A), which ubiquitylates p53 [6-8]. In promoting  
75 the ubiquitin dependent proteolysis of p53, E6 counters E7-mediated replication stress  
76 signals that activate and stabilize p53 [9]. Thus, inhibition of the E6/E6AP-mediated  
77 ubiquitylation of p53 is proapoptotic and provides a potential validated target for HPV-  
78 positive cancers. Direct targeting of E6 induces apoptosis in HPV-positive cancer cells [10].  
79 Although the hrHPV E6 proteins have other cellular activities and protein targets that have  
80 been described in the literature, we have focused on the E6/E6AP pathway as a potential  
81 therapeutic target for HPV-positive cancers, as well as precancerous lesions.

82 MicroRNAs (miRNAs/miRs) are small non-coding RNAs (approximately 22 nucleotides in  
83 length) that significantly impact and regulate many essential biological pathways. miRNAs  
84 negatively regulate gene expression either by translational repression of the target mRNA  
85 or cleavage of target mRNAs. Many miRNAs have been shown to play roles in cancer,  
86 sometimes as oncogenes and other times as tumor suppressors, making them suitable as  
87 therapeutic targets. miRNAs themselves can be used as cancer therapeutics, as their ectopic

88 expression may affect one or more pathways essential for the replication and survival of  
89 specific cancer cells. There have been a number of studies focused on HPV and miRNAs in  
90 recent years. These studies have examined whether HPVs, like many other viruses, encode  
91 viral miRNAs [11] and whether the HPV oncoproteins regulate the expression of cellular  
92 miRNAs [12]. Other studies have proposed miRNAs as potential biomarkers of hrHPV  
93 infections [13]. There have also been some studies that have examined the effect of miRNA  
94 expression in various cancers including cervical cancers (For review see [14]). It was with  
95 this mindset, that we conducted a screen to identify miRNAs whose expression in HPV-  
96 positive cancer cells would stabilize p53.

97 Here we describe a cell-based platform to assay p53 stability in hrHPV E6-expressing HeLa  
98 cells and present our results from a high-throughput screen that identified microRNAs  
99 whose expression increased p53 protein levels and caused apoptosis. To our knowledge  
100 this is the first study to systematically exam miRNAs for their abilities to stabilize p53 in  
101 hrHPV-positive cancer cells. As result of this screen, we have identified a number of  
102 miRNAs that when ectopically expressed in these cells lead to increased levels of p53. We  
103 also provide insights into the mechanisms by which some of these miRNAs function in  
104 stabilizing p53 and apoptosis induction.

## 105 **Results**

106 **A high-throughput screen identified miRNAs whose**  
107 **overexpression stabilizes p53 in HeLa cells.**

108 To identify miRNAs whose overexpression stabilizes p53 and induces apoptosis in hrHPV-  
109 positive cancer cells, we performed a high-throughput screen in HPV18-positive HeLa cells  
110 harboring a reporter for p53 protein stability. The reporter expresses a bicistronic mRNA  
111 that encodes an EGFP-p53 fusion protein and the red fluorescent protein DsRed as  
112 reference (Fig 1A). In this screen, we used the p53 gene encoding the R273C mutated  
113 protein, which is targeted by E6/E6AP for ubiquitin-dependent proteolysis [15]. This  
114 mutant acts as a dominant negative interfering with the transcriptional activities of the  
115 endogenous wild-type (wt) p53, thereby preventing p53 transcriptionally-driven apoptosis  
116 triggered by the eventual stabilization of the endogenous p53 during the course of the  
117 assay. The stability of the EGFP-p53(R273C) fusion protein is controlled by the less stable  
118 protein, in this case p53, with a half-life less than 30 minutes in HeLa cells due to E6-  
119 mediated proteolysis [5, 16]. To detect changes in p53 stability, we monitored the  
120 EGFP/DsRed fluorescence ratio by laser scanning cytometry. The results of this screen,  
121 which assayed 885 miRNAs, are shown in S1 Table. The top hit (375-3p) was previously  
122 reported to stabilize p53 in HPV-positive cells [17] and thus provided validation for the  
123 screen. Of note, since all the miRNAs used in this study are human, we omitted the use of  
124 the prefix hsa-miR in the miRNAs names. We selected for further testing the miRNAs that  
125 produced the next 32 highest EGFP/DsRed fluorescence ratios (Table 1). Sequence analysis  
126 of the selected miRNAs showed a significant enrichment of miRNAs sharing a common seed  
127 sequence (5'-AAGUGC-3') that defines the 302-3p/372-3p/373-3p/519-3p/520-3p family  
128 of miRNAs (302/519 miRNA family) (S1 Fig). Three additional miRNAs from this family  
129 (302d-3p, 520a-3p, and 520e-3p) that had EGFP/DsRed fluorescence ratios close to the  
130 selected 32 miRNAs were also included for further evaluation.

131 **Table 1. miRNAs selected from primary screen**

132

Rank	miRNA	Mature_Sequence	EGFP / DsRed (Mean, n = 3)	EGFP / DsRed (SD, n =3)
1	hsa-miR-375-3p	UUUGUUCGUUCGGCUCGCGUGA	0.12298	0.01761
2	hsa-miR-219a-5p	UGAUUGUCCAACGCAAUUCU	0.07703	0.00559
3	hsa-miR-511-5p	GUGUCUUUUGCUCUGCAGUCA	0.07371	0.00962
4	hsa-miR-519c-3p	AAAGUGCAUCUUUUUAGAGGAU	0.0718	0.0169
5	hsa-miR-943	CUGACUGUUGCCGUCCUCCAG	0.06086	0.02073
6	hsa-miR-200c-5p	CGUCUUACCCAGCAGUGUUUGG	0.05781	0.0079
7	hsa-miR-944	AAAUUAUUGUACAUCGGAUGAG	0.05766	0.03304
8	hsa-miR-106a-3p	CUGCAAUGUAAGCACUUCUAC	0.0521	0.00779
9	hsa-miR-374b-5p	AUAUAAUACAACCUGCUAAGUG	0.05065	0.00389
10	hsa-miR-148b-5p	AAGUUCUGUUAUACACUCAGGC	0.05013	0.00438
11	hsa-miR-519d-3p	CAAAGUGCCUCCUUUAGAGUG	0.04929	0.01507
12	hsa-miR-631	AGACCUGGCCAGACCUCAGC	0.04839	0.01369
13	hsa-miR-592	UUGUGUCAUAUGCGAUGAUGU	0.0469	0.0122
14	hsa-miR-519b-3p	AAAGUGCAUCCUUUUAGAGGUU	0.04442	0.01903
15	hsa-miR-93-3p	ACUGCUGAGCUAGCACUCCCG	0.04441	0.00884
16	hsa-miR-340-5p	UUAUAAAGCAAUGAGACUGAUU	0.04336	0.00383
17	hsa-miR-508-3p	UGAUUGUAGCCUUUUGGAGUAGA	0.04083	0.00853
18	hsa-miR-374a-3p	UUAUAAUACAACCUGAUAAGUG	0.03978	0.00887
19	hsa-miR-520d-3p	AAAGUGCUUCUCUUUGGUGGGU	0.0379	0.01428
20	hsa-miR-520c-3p	AAAGUGCUUCCUUUUAGAGGGU	0.0329	0.01176
21	hsa-miR-520b-3p	AAAGUGCUUCCUUUUAGAGGG	0.03226	0.01171
22	hsa-miR-153-3p	UUGCAUAGUCACAAAAGUGAUC	0.03096	0.00799
23	hsa-miR-17-5p	CAAAGUGCUUACAGUGCAGGUAG	0.02945	0.01485
24	hsa-miR-519a-3p	AAAGUGCAUCCUUUUAGAGUGU	0.02878	0.00725
25	hsa-miR-1287-5p	UGCUGGAUCAGUGGUUCGAGUC	0.02854	0.00375
26	hsa-miR-373-3p	GAAGUGCUUCGAUUUUGGGGUGU	0.028	0.00787
27	hsa-miR-302a-3p	UAAGUGCUCCAUGUUUUGGUGA	0.02791	0.00701
28	hsa-miR-302b-3p	UAAGUGCUCCAUGUUUAGUAG	0.02749	0.01175
29	hsa-miR-509-3p	UGAUUGGUACGUCUGUGGGUAG	0.02568	0.00559
30	hsa-miR-210-3p	CUGUGCGUGUGACAGCGGCUGA	0.0256	0.00996
31	hsa-miR-302c-3p	UAAGUGCUCCAUGUUUCAGUGG	0.02376	0.00492
32	hsa-let-7a-2-3p	CUGUACAGCCUCCUAGCUUCC	0.02275	0.01039
33	hsa-miR-224-5p	CAAGUCACUAGUGGUUCCGUU	0.0223	0.00997
35	hsa-miR-302d-3p	UAAGUGCUCCAUGUUUGAGUGU	0.02153	0.00361
42	hsa-miR-520e-3p	AAAGUGCUUCCUUUUUGAGGG	0.01761	0.00714
44	hsa-miR-520a-3p	AAAGUGCUUCCUUUGGACUGU	0.01673	0.0059

133

134



135 To confirm the results obtained in the screen, we tested the selected miRNAs in HeLa cells  
136 containing a different bicistronic reporter vector (Fig 1B) in which p53(R273C) is fused to  
137 mRuby, a bright monomeric red fluorescent protein, and the reference monomeric green  
138 fluorescent protein SGFP2 is fused to H2B [18]. In this experiment, we determined the  
139 percentage of H2B-SGFP2 expressing cells that also expressed mRuby-p53 (R273C) using  
140 flow cytometry. We used two randomly selected miRNAs (498-5p and 665), which were  
141 negative in the initial screen, and the miRNA Ctrl. 1 as negative controls, along with 375-3p  
142 as a positive control. As shown in S2 Fig, 27 of the 32 originally selected miRNAs were  
143 confirmed to also stabilize mRuby-p53 (R273C) in this reporter HeLa cell line.

## 144 **Validation of candidate miRNAs in HeLa cells**

145 The 27 confirmed miRNAs were next tested for their ability to stabilize endogenous p53 in  
146 HeLa cells as determined by western blotting (Figs 2 and S3). While transfection of most of  
147 the miRNAs resulted in some degree of p53 stabilization compared to the mock and  
148 negative controls, four miRNAs (219-5p, 106a-3p, 592, and 508-3p) had little or no effect  
149 on endogenous p53 levels. The other miRNAs ranged from those that produced a mild to  
150 moderate increase in p53 levels (511-5p, 519d-3p, 631, 374a-3p, 153-3p, 17-5p, 373-3p,  
151 210-3p, and 302c-3p) to those that caused stronger p53 stabilization (519c-3p, 943, 374b-  
152 5p, 148b-5p, 519b-3p, 93-3p, 520d-3p, 520c-3p, 520b-3p, 519a-3p, 302a-3p, 302b-3p, 509-  
153 3p, and 1287-5p). We also examined the effects of the miRNAs on E6AP and HPV18 E6  
154 protein levels. Although most miRNAs had little or no effect on E6AP levels, miRNAs 148b-  
155 5p, 374a-3p, and 374b-5p decreased the levels of E6AP to values similar to those observed  
156 in cells transfected with the positive control 375-3p, which has been previously shown to  
157 target the E6AP mRNA [17]. Transfection of a few miRNAs, most notably 93-3p and 1287-

158 5p, resulted in elevated levels of E6AP (Figs 2 and S3). In contrast, transfection of most of  
159 the tested miRNAs led to a reduction in E6 protein levels (Figs 2 and S3). While there was  
160 no correlation between the protein levels of E6 and E6AP or between E6AP and p53, there  
161 was a significant negative correlation between the levels of E6 and p53, suggesting that a  
162 decrease in E6 expression plays a significant role in the stabilization of p53 by several of  
163 these miRNAs in HeLa cells (S4 Fig). A ~50% reduction in E6 protein levels appears  
164 necessary for p53 stabilization in these cells. Based on these results, we selected miRNAs  
165 148b, 374a, 374b, 1287, and five members of the 302/519 family for further analysis.

## 166 **Expression of selected miRNAs increase levels of p53 in** 167 **different cell lines.**

168 To study the effect of this set of miRNAs on the stability of p53 in other hrHPV-positive  
169 cancer cell lines, we transfected SiHa (HPV16), ME-180 (HPV68), and MS751 (HPV45) cells  
170 with the selected miRNAs and examined p53, E6AP, and actin protein levels by western  
171 blot. As shown in Fig 3A-C, the expression of these miRNAs increased the protein levels of  
172 p53 in all three cell lines, although with varying efficiencies, indicating that the p53  
173 stabilization effect was independent of the hrHPV type.

174 To evaluate the involvement of the E6/E6AP pathway in the stabilization of p53 by these  
175 miRNAs, we examined their effects on the levels of p53 and E6AP in HPV-negative human  
176 U2OS cells (Fig 3E), an osteosarcoma-derived cell line that harbors wt p53 under the  
177 control of Mdm2. Transfection of miRNAs 375-3p and 148b-5p increased the levels of p53  
178 in U2OS cells (Fig 3E), indicating that these two miRNAs affect p53 protein levels  
179 independent of HPV oncoprotein expression. In contrast, ectopic expression of the miRNAs

180 from the 302/519 family and 1287-5p had no effect on the levels of p53 in U2OS cells,  
181 suggesting that the effect of these miRNAs on p53 stability depends on the expression of  
182 hrHPV E6. Of note, transfection of miRNAs 375-3p, 148b-5p and to a lesser degree 374a-3p  
183 and 374b-5p, decreased the levels of E6AP in each of the cell lines analyzed. As expected,  
184 no miRNA produced a significant change in p53 levels in the HPV-negative C33A cervical  
185 cancer cell line that already expresses high levels of an inactive mutant form of p53 (Fig  
186 3D) [19].

187 Since transfection of the 302/519 family members and 1287-5p miRNAs only increased  
188 p53 levels in HPV-positive cells and led to decreased E6 protein levels in HeLa cells, which  
189 negatively correlated to the levels of p53 (Figs 2 and 4S), we hypothesized that the ability  
190 of these miRNAs to stabilize p53 in HPV-positive cancer cells was a direct consequence of  
191 their effect on E6 expression. This could be a consequence of destabilizing the E6 protein,  
192 targeting the E6/E7 mRNAs for degradation or sequestration, or decreasing viral  
193 transcription. To explore these possibilities, we examined the effect of the miRNAs on the  
194 levels of p53 in 1321 cells, a human keratinocyte cell line that expresses HPV16 E6/E7  
195 under the control of the human  $\beta$ -actin promoter and from a mRNA with the 3'  
196 untranslated region (3'UTR) of the human  $\beta$ -actin mRNA [20] (Fig 3D). While transfection  
197 of miRNAs 375-3p, 148b-5p, 374a-3p, and 374b-5p stabilized p53, ectopic expression of  
198 miRNAs of the 302/519 family and 1287-5p produced little to no change on p53 levels in  
199 1321 cells. This indicates that stabilization of p53 by the miRNAs of the 302/519 family  
200 and 1287-5p in HPV-positive cervical cancer cell lines is likely mediated by reduced E6  
201 expression from the viral long control region (LCR) promoter.

## 202 **Several miRNAs repress the promoter activity of the HPV16 and** 203 **18 LCRs.**

204 The hrHPV E6 and E7 genes are expressed from a single promoter located in the viral LCR.  
205 Consistent with the hypothesis that these miRNAs affect the promoter activity of the viral  
206 LCRs, we observed that their transfection into HeLa cells, particularly the members of the  
207 302/519 family and 1287-5p, decreased both E6 and E7 protein levels similarly (Fig 4A).  
208 To examine whether these selected miRNAs repressed promoter activity of the HPV LCRs,  
209 we used reporter plasmids that express firefly luciferase under the control of either the  
210 HPV16 or HPV18 LCR (Fig 4B). Remarkably, with the exception of 148b-5p, all of the  
211 miRNAs tested repressed the LCR-dependent expression of firefly luciferase in C33A cells.  
212 Most miRNAs showed a comparable effect on both LCRs, except 374b-5p, which did not  
213 significantly repress the HPV16 LCR. Expression of the 302/519 family members and 1287-  
214 5p led to the greatest repression of both HPV16 and HPV18 LCRs.

215 We next used qRT-PCR to directly assess the impact of these miRNAs on the levels of HPV  
216 E6/E7 mRNAs in HeLa and SiHa cells (Fig 4C). Using primers that detect all HPV E6/E7  
217 transcripts, we observed a significant reduction of the E6/E7 mRNAs upon transfection  
218 with each of the miRNAs except 148b-5p in HeLa cells, indicating regulation of E6 and E7  
219 expression at a pre-translational level. Although 498-5p reduced the level of the E6/E7  
220 mRNAs in HeLa cells, consistent with the reduced level of E6 protein shown in Fig 2, we did  
221 not observe an increase in p53 protein levels in these cells (see discussion). While 375-3p  
222 was equally efficient in repressing the expression of the E6/E7 mRNAs in both HPV-  
223 positive cell lines, most of the tested miRNAs were less efficient in SiHa than in HeLa cells

224 even though SiHa cells were efficiently transfected as determined by siGlo RISC-free  
225 transfection control (Horizon). Surprisingly, transfection of 148b-5p increased the level of  
226 the E6/E7 mRNAs in both cell lines suggesting that neither downregulation of the  
227 promoter activity of the LCR nor destabilization of the E6/E7 mRNAs contribute to the  
228 stabilization of p53 by this miRNA in these cells. We also observed that transfection of 375-  
229 3p, which efficiently reduced the E6/E7 mRNAs levels in both HeLa and SiHa cells, has a  
230 milder effect on both viral promoters compared to the miRNAs of the 302/519 family or  
231 1287-5p, indicating that, as published by others, 375-3p also affects the levels of the E6/E7  
232 mRNAs post-transcriptionally [17]. A similar observation can be made for 374a-3p and  
233 374b-5p in HeLa cells. In general, in HeLa cells, there is a correlation between the levels of  
234 E6 protein and E6/E7 mRNAs with the degree of repression of the viral promoter,  
235 suggesting that downregulation of the LCR promoter is an important factor in the  
236 regulation of E6 expression by the tested miRNAs in these cells. In contrast, in SiHa cells,  
237 with the exception of 148b-5p, there was little or no correlation between the levels of the  
238 E6/E7 mRNAs and the degree of repression of the viral promoter. This indicates that, in  
239 addition of repressing the LCR promoter activity, other factors likely contribute to the E6  
240 downregulation and p53 stabilization by these miRNAs in SiHa cells.

241 **miRNAs of the 302/519 family and 1287-5p induce p53-**  
242 **dependent apoptosis in HeLa cells.**

243 Stabilization of p53 is expected to be pro-apoptotic in hrHPV-positive cells. We therefore  
244 tested the miRNAs that stabilized p53 in HeLa cells for their abilities to induce apoptosis.  
245 Flow cytometry analysis of HeLa cells transfected with different miRNAs and stained with

246 the apoptosis marker Annexin V revealed an increase in the fraction of apoptotic cells when  
247 compared to untreated or mock transfected cells (Fig 5). Surprisingly, miRNAs Ctrl.1 and  
248 498-5p, which did not increase p53 levels in hrHPV positive cells (Figs 2 and 3) also led to  
249 an increase in Annexin V staining in HeLa cells. In addition, we noticed a strong correlation  
250 between induction of apoptosis, stabilization of p53 (Fig 2), and repression HPV18 LCR (Fig  
251 4B) in HeLa cells transfected with the 302/519 family members. In this family, 519d-3p,  
252 which produced the lowest increase in p53 level in HeLa cells, was also the least efficient in  
253 inducing apoptosis.

254 We next examined the ability of a subset of these miRNAs to induce apoptosis in SiHa cells  
255 and two HPV-negative cancer cell lines, C33A and U2OS, using Annexin V staining (Fig 6).  
256 Because the negative controls Ctrl. 1 and 498-5p induced apoptosis in HeLa cells (Fig 5), we  
257 included the miRNA 20a-3p as a negative control since it has been previously reported not  
258 to induce apoptosis in cervical cancer cells [21]. The 1287-5p miRNA was also included in  
259 these experiments as it was found to stabilize p53 (Figs 2 and 3) and efficiently repressed  
260 the E6/E7 mRNAs expression in HeLa and SiHa cells as well as the promoter activity of the  
261 HPV16 and HPV18 LCR reporters (Fig 4B and 4C). Similar to our results in HeLa cells,  
262 148b-5p and 1287-5p induced apoptosis in SiHa cells whereas 375-3p and 519b-3p had  
263 very little or no effect (Fig 7). All of these miRNAs increased the levels of p53 when  
264 transfected into SiHa cells (Fig 3A); however, 148b-5p and 1287-5p led to the highest p53  
265 levels. Both 148b-5p and 1287-5p stimulated apoptosis in C33A cells indicating that these  
266 miRNAs can induce apoptosis independently of p53.

267 We next examined the requirement for p53 stabilization in the induction of apoptosis in  
268 HeLa cells for several representative miRNAs. We performed Annexin V staining of HeLa

269 cells co-transfected with the miRNAs and an siRNA targeting p53 or its C911 variant [22] to  
270 address possible off-target effects of the siRNA (Fig 7A). As expected, the positive control  
271 375-3p increased the percentage of Annexin V-stained cells while 20a-3p had no significant  
272 effect when compared to untreated cells. Surprisingly, the apoptotic effect of 375-3p was  
273 independent of p53 since knock-down of p53 had little effect on the percentage of  
274 apoptotic cells in HeLa cells co-transfected with this miRNA. The effect of 498-5p on  
275 apoptosis is also p53-independent and consistent with the inability of this miRNA to  
276 stabilize p53 when transfected into hrHPV-positive cell lines (Figs 2 and 3). Similarly, the  
277 apoptotic effects of miRNAs 148b-5p and 374a-3p are p53-independent, as co-transfection  
278 of these miRNAs with either the siRNA against p53 or its C911 version have similar effects  
279 on the percentage of apoptotic cells. This indicates that, in these cases, the effect observed  
280 when p53 is knocked down can be attributed to off-target effects of the siRNA against p53.  
281 In contrast, the numbers of apoptotic cells observed with 519b-3p (as a representative of  
282 the 302/519 family of miRNAs) and 1287-5p were reduced when co-transfected with the  
283 p53 siRNA but not with its C911 version, indicating that the apoptotic effect of these  
284 miRNAs is largely p53-dependent in HeLa cells. Similar results were obtained when using  
285 PARP cleavage as a marker for apoptosis in western blot analysis (Fig 7B). Altogether,  
286 these results showed that expression of the selected miRNAs induces apoptosis in HeLa  
287 cells via mechanisms that are either independent of p53 protein levels, as in the case of  
288 148b-5p and 374a-3p, or p53-dependent, as found with 519b-3p and 1287-5p.

## 289 Discussion

290 In this manuscript, we describe a platform that can be used in a high-throughput manner  
291 (e.g. siRNA, CRISPR-Cas9, and small molecule screens) to monitor p53 stability *in vivo* in  
292 HPV-positive cancer cells. Here we present our results using this platform to screen a  
293 library of miRNA mimics in HeLa cells to find candidates whose overexpression stabilized  
294 p53 in hrHPV-positive cancer cells. We identified several miRNAs that increased the  
295 protein levels of p53 when transfected in HeLa cells. Some of these miRNAs (148b-5p,  
296 302a-3p, 373-3p, and 374b-5p) have been reported to be expressed at lower levels in  
297 cervical cancer cells and tissues compared to the controls used in each of the studies [21,  
298 23-25]. In contrast, 1287-5p has no change in its expression level in cervical cancer cells,  
299 but is sequestered from its targets by the circular RNA circSLC26A4, which is  
300 overexpressed in hrHPV-positive cancer cells [26]. In addition, some of the miRNAs  
301 identified in our screen, namely 148b-5p, 302a-3p, 374b-5p, or 519b-3p, have already been  
302 shown to have effects in hrHPV-positive cervical cancer cells affecting cellular behavior,  
303 slowing cell growth and inducing apoptosis [23-25, 27, 28]. Although several targets and  
304 mechanisms have been shown to contribute to these effects, there is little data about how  
305 the ectopic expression of these miRNAs affects E6, E6AP and p53 expression, nor the  
306 possible consequences of changes in the expression E6, E6AP, and p53 in the ability of  
307 these miRNAs to induce apoptosis in hrHPV-positive cervical cancer cells.  
308 Since the ubiquitin ligase activity of E6AP/E6 is responsible for the efficient ubiquitin-  
309 dependent proteolysis of p53 in hrHPV-positive cervical cancer cells, we checked the levels  
310 of E6AP in cells transfected with the different miRNAs. Interestingly, only four miRNAs,  
311 148b-5p, 374a-3p, 374b-5p, and 375-3p, were identified that led to a decrease in E6AP



312 protein levels. Remarkably, the three miRNAs of this group that were further analyzed  
313 (148b-5p, 374a-3p, and 375-3p) increased apoptosis in HeLa cells in a p53-independent  
314 manner. It is possible that this induction of apoptosis may still be HPV-related, as these  
315 miRNAs also led to decreased E6 protein expression. However, 148b-5p induced apoptosis  
316 in the absence of the HPV oncoproteins as observed in C33A cells and both 375-3p and  
317 148b-5p stabilized p53 in HPV-negative U2OS cells. These results indicate that these  
318 miRNAs can affect p53 protein levels independent of their effect on E6. Although we did not  
319 determine whether they directly target the E6AP mRNA, it seems probable for both 148b-  
320 5p and 374b-5p because target prediction analysis using the miRDB database  
321 ([www.mirdb.org](http://www.mirdb.org)) [29, 30] revealed that each has three sites complementary to their seed  
322 sequences within the 3'UTR of the E6AP mRNA. They start at positions 395, 664, and 1595  
323 of the 3'UTR for 148b-5p, and at positions 236, 908, and 1334 for 374b-5p.  
324 In contrast, our results indicate that 519b-3p (member of the 302/519 family) and 1287-  
325 5p induce apoptosis in HeLa cells in a p53-dependent manner. Our observations do not  
326 fully align with previous reports that indicated transfection of 519b-3p increases p21 levels  
327 in a partly p53-independent manner, resulting in growth inhibition and cell survival, while  
328 failing to induce cell death [28]. There are a number of technical differences between our  
329 study and that of Abdelmohsen et al. which could account for the discordant results.  
330 Different concentrations of miRNAs were used in each study (50 nM in the Abdelmohsen  
331 study and 10 nM in our study) and their analyses were done at 48 hours post-transfection  
332 whereas our studies were conducted at 72 hours post transfection.  
333 Although there are sequences complementary to the seed sequence of miRNAs of the  
334 305/519 family in the 3'UTR of the E6AP mRNA (starting at positions 934 and 935 of the

335 3'UTR) we did not observe any significant effect on E6AP expression levels in the various  
336 cell lines transfected with these miRNAs. However, it has recently been reported that 302c-  
337 3p, which belongs to this family, regulates the expression of E6AP by targeting the 3'UTR of  
338 the E6AP mRNA in hepatic stellate cells [31]. Again, methodological differences between  
339 the two studies, most notably the cell type used, could explain the different findings. It is  
340 feasible that the cells differ in availabilities of the target sequence in the 3'UTR of the E6AP  
341 mRNA for the miRNAs of the 302/519 family, for example by differential expression of an  
342 RNA-binding protein that could compete with the miRNAs for binding to the target  
343 sequence [32]. In addition, the concentration of miRNA used by Kim et al. was 100 nM, ten  
344 times higher than that used in our study. Overexpression of miRNAs can produce a series of  
345 confounding effects (reviewed in [33]), such as binding to lower-affinity targets that are  
346 not affected by lower miRNA concentrations. At a concentration of 10 nM we found that the  
347 miRNAs of the 302/519 family stabilize p53 but do not impact E6AP expression in cervical  
348 cancer cells. The fact that they can stabilize p53 at relatively low concentrations makes  
349 them more attractive as potential therapeutics for cervical cancer by reducing potential  
350 side effects due to targeting of low affinity sites.

351 Different viral processes affected by host miRNAs have been described (reviewed in [34]);  
352 however, miRNAs affecting the activity of viral promoters are not commonly found in the  
353 literature. Transfection of 302/519 family members or 1287-5p led to increased protein  
354 levels of p53 only in cells in which E6 and E7 expression is driven by viral LCRs (HeLa,  
355 SiHa, ME-180, and MS751). This suggests that the effect of these miRNAs on E6 and E7  
356 expression may involve a reduction in the activity of the viral promoters. Here we showed  
357 that ectopic expression of these miRNAs efficiently repressed the activity of the HPV16 and

358 HPV18 LCRs in C33A cells expressing LCR/luciferase reporters and resulted in decreased  
359 E6/E7 mRNAs levels in both HeLa and SiHa cells. It is possible that these miRNAs target  
360 transcription factors that regulate HPV LCR promoter activities. We note that although  
361 375-3p has been reported to target E6/E7 mRNAs in HeLa and SiHa cells [17], our data  
362 show that 375-3p also decreases the expression levels of E6 and E7 by repressing the  
363 promoter activity of the viral LCRs. This might involve the downregulation of the  
364 transcription factor SP1 by 375-3p [35], which is key for the activity of the promoter  
365 driving E6 and E7 expression in hrHPVs [36, 37]. In terms of the 302/519 miRNA family  
366 members, 519a-3p and 519d-3p have been shown to target signal transducer and activator  
367 of transcription 3 (STAT3) mRNA [38, 39], which is another driver of HPV gene expression  
368 [40]. Noteworthy, knocking down or inhibiting STAT3 in hrHPV-positive cervical cancer  
369 cell lines led to loss of E6 and E7 expression, accumulation of p53, and reduced cell viability  
370 [41]. The similarities between the effects of ectopic expression of the 302/519 family of  
371 miRNAs and STAT3 depletion in hrHPV-positive cancer cells make STAT3 an interesting  
372 candidate to mediate the effects of these miRNAs in hrHPV-positive cells. Another  
373 possibility is that these miRNAs regulate the LCR promoter activity through direct binding  
374 to viral or host DNA as it has been described for other miRNAs [42]. Though we could not  
375 find any evident sequence similarities to these miRNAs in the HPV16 and HPV18 genomes,  
376 we cannot fully exclude this possibility. These are all interesting questions that will be  
377 addressed in future studies.

378 Both the 302/519 family members and 1287-5p induced apoptosis in HeLa cells. In the  
379 case of 519b-3p (as representative of the 302/519 family of miRNAs) and 1287-5p this  
380 induction was p53-dependent. Surprisingly, 519b-3p failed to induce apoptosis in SiHa

381 cells despite increasing the levels of p53. It has been previously reported that p53 must  
382 accumulate to a threshold level to induce apoptosis [43]. Thus, it is feasible that for 519b-  
383 3p the concentration of miRNA and/or incubation times used in this study did not increase  
384 p53 levels enough to reach the critical threshold necessary to trigger apoptosis in SiHa  
385 cells. A similar reasoning could be applied to 148b-5p, which failed to induce apoptosis in  
386 U2OS cells despite the stabilization of wt p53 (Fig 3E). In contrast, 1287-5p induced  
387 apoptosis in U2OS cells without a noticeable increase in p53 levels, indicating that in these  
388 cells this miRNA promotes cell death independent of p53 stabilization. This suggests that  
389 1287-5p can induce apoptosis via different pathways depending on cell type, highlighting  
390 the risk of extrapolating miRNA effects observed in one cell line to different cell types. Of  
391 note, transfection of 498-5p, which was initially chosen as a negative control because it did  
392 not stabilize p53 in HeLa cells, resulted in decreased levels of E6 in these cells. This  
393 suggests that either the remaining E6 protein was sufficient to target p53 for degradation  
394 or that 498-5p has the additional property of inhibiting p53 accumulation. However, in this  
395 study, the miRNAs that failed to reduce E6 protein levels to approximately half of its  
396 original amount or beyond also failed to increase p53 levels in HeLa cells, suggesting that  
397 there is a considerable excess of E6 in these cells that must be overcome in order to  
398 stabilize p53. Interestingly, ectopic expression of Ctrl. 1 stabilized p53 only in U2OS cells,  
399 further demonstrating how an individual miRNA affects different cell types in distinct  
400 ways.

401 A match of the seed sequence of the miRNAs is very important for target recognition [44,  
402 45]. However, it has been reported that additional pairing to 3' sequences of miRNAs  
403 frequently participate in target site recognition and avidity, resulting in different target

404 specificities for miRNAs of a given miRNA family [46]. In this study we found that different  
405 members of the 302/519 family of miRNAs, all with the same seed sequence, differed in the  
406 extent to which p53 protein levels increased, indicating that 3' miRNA sequences may also  
407 play a role in their stabilization of p53 in hrHPV-associated cancer cells. Regardless, the  
408 common seed sequence of the miRNAs within the 302/519 family that we found to repress  
409 the HPV18 and HPV16 LCR promoters is a characteristic that can be used to identify their  
410 potential targets involved in viral LCR promoters regulation.

411 Since their discovery in 1993 [47, 48], there has been a major and growing interest in  
412 miRNAs. A PubMed search for articles with “microRNA” or “miRNA” in the title reveals  
413 more than 41,000 publications. Research in miRNAs is being translated into diagnostics as  
414 miRNAs are considered sensitive and specific biomarkers whereas therapeutic  
415 opportunities with miRNAs have lagged with only a few clinical trials currently in progress  
416 (reviewed in [49, 50]). This may in part be due to the lack of single target specificity  
417 characteristic of miRNAs. This multiplicity of targets makes miRNAs potentially challenging  
418 as therapeutics because of the possibility of unexpected and/or undesirable side effects.

419 However, this property makes them an attractive tool for cancer treatment since miRNAs  
420 can simultaneously regulate multiple cellular pathways by modulating the expression of  
421 several genes in a coordinated fashion. The utility of miRNAs as therapeutic tools will be  
422 improved by a more complete understanding of how they function in the cellular networks  
423 in which they are embedded. In this study, we identified several miRNAs that stabilize p53  
424 and can induce apoptosis, both in a p53-dependent or p53-independent manner, when  
425 ectopically expressed in hrHPV-positive cancer cells. Most of these miRNAs function  
426 through transcriptional repression of the HPV LCR promoter, especially 519b-3p and 1287-

427 5p. Further research on the mechanisms used by these miRNAs to repress the hrHPV LCRs  
428 and induce apoptosis in HPV-positive cervical cancer cells will improve our understanding  
429 of the hrHPV-host interactions and possibly contribute to the identification of new  
430 therapeutic targets for hrHPV infections and cancers.

## 431 **Materials and methods**

### 432 **Plasmids**

433 To create a lentiviral reporter vector to monitor the protein levels of p53 *in vivo* in hrHPV  
434 cancer cells, the p53 open reading frame (ORF) carrying the mutation R273C was first  
435 amplified by PCR using the primers hp53-1 (5'-CACCATGGAGGAGCCGCGAGTCAGATCC-3')  
436 and hp53-8 (5'-GGATCCTCAGTCTGAGTCAGGCCCTTCTGTCTTG-3') and cloned into the  
437 pENTR/D-TOPO vector (ThermoFisher) generating the entry vector pENTR p53(R273C)  
438 (p6140). The p53(R273C) ORF was then recombined from the entry vector into a lentiviral  
439 vector containing a GPS (Global Protein Stability) cassette (gift from S. Elledge) using the  
440 GATEWAY cloning system (ThermoFisher), resulting in the vector pHAGE-P CMVt N-RIG2  
441 p53(R273C) (p7987). The GPS reporter cassette expresses a bicistronic mRNA encoding  
442 EGFP fusion proteins and the red fluorescent protein DsRed as reference (Fig 1A) [51-54].  
443 The reporter vector pHAGE-N CMVt N-RIG3 p53(R273C) (p7709), which contains a variant  
444 of the GPS reporter cassette, expresses p53(R273C) fused to the monomeric red  
445 fluorescent protein mRuby and a monomeric green fluorescent protein (SGFP2) fused to a  
446 histone 2B (H2BC11) as reference (Fig 1A) [18]. The vectors pGL4.20-HPV16-LCR-  
447 luciferase (p6239) and pGL4.20-HPV18-LCR-luciferase (p5194), expressing the firefly  
448 luciferase under the control of the HPV16 and HPV18 LCRs respectively, have been

449 previously described [55]. Renilla luciferase was amplified from pRL-TK-Rluc (Promega #  
450 E2241 - GenBank® Accession Number AF025846) using the primers 5'-  
451 CAAGTCGACATGACTTCGAAAGTTTAT-3' and 5'-CTTAAGCTTATTGTTTCATTTTTGAGAA-3',  
452 and cloned into the p1318 human  $\beta$ -actin-based mammalian expression plasmid, which  
453 contains a 4.3-kilobase EcoRI-AluI human  $\beta$ -actin promoter fragment, the human  $\beta$ -actin 3'  
454 untranslated region, poly(A) site, and 3' flanking region [20] to generate (p7988).

## 455 **Cell lines**

456 HeLa, HeLa GPS p53(R273C), HeLa RIG3 p53(R273C), Siha (ATCC® HTB-35™), C33A  
457 (ATCC® HTB-31™), U2OS (ATCC® HTB-96™), ME-180 (ATCC® HTB-33™), MS-751  
458 (ATCC® HTB-34™), and human keratinocytes immortalized by HPV16 E6 and E7 expressed  
459 from the  $\beta$ -actin promoter (p1321) [20] referred to here as 1321 cells were grown in  
460 Dulbecco's modified Eagle's medium (DMEM) supplemented with 10% (v/v) fetal bovine  
461 serum at 37°C 5% CO<sub>2</sub>.

## 462 **miRNA screen**

463 For the primary miRNA screen, HeLa GPS p53(R273C) cells were reverse transfected with  
464 the Ambion Human Pre-miR miRNA Mimic Library (2009) based on miRBase release 13.0.  
465 in a one-target, one-well format using 384-well microtiter plates in a high-throughput  
466 format. The Z'-factor [56] was calculated for each assay plate and was consistently > 0.6,  
467 indicating assay robustness. siRNA buffer (1×) (Horizon #B-002000-UB-100) was  
468 aliquoted into wells, miRNA mimics were added so that the final concentration was 40  
469 nM/well, and DharmaFECT1/OptiMEM was dispensed into wells. While the miRNA/lipid  
470 mix was allowed to complex, cells were trypsinized, counted, and resuspended to reach a

471 plating density of 600 cells/well. Cells were seeded on top of the miRNA/lipid mixture,  
472 briefly centrifuged, and incubated for 72 hours, a time that we determined to be optimal for  
473 p53 stabilization for small miRNAs. The cells were then equilibrated to room temperature  
474 (~15 min) before analysis. Using TTP LabTech's Acumen eX3 laser scanning cytometer, the  
475 total EGFP and DsRed intensities in each well were quantitated. Internal controls were  
476 present in Columns 13 and 14 of each library plate (Pre-miR miRNA Precursor Molecules  
477 Negative Control #1 - Ambion AM171110; Pre-miR miRNA Precursor Molecules Negative  
478 Control #2 - Ambion AM171111; PLK1 SMARTpool Dharmacon M-003290-01). In addition,  
479 siRNAs against E6AP (UBE3A, Dharmacon D-005137-04) and non-targeting siRNAs  
480 (Dharmacon D-001210-01 and D-001210-02) were added to each plate. The miRNA  
481 mimics were screened in triplicate. High-throughput libraries and screening capability was  
482 provided by the ICCB-Longwood Screening Facility at Harvard Medical School.

### 483 **miRNA transfections**

484 All cells were reverse transfected with miRNAs (S2 Table) using RNAiMax according to  
485 manufacturer's instructions (ThermoFisher Scientific). More specifically, 750  $\mu$ l of  
486 suspended cells were added to 250  $\mu$ l of a transfection mix containing 2  $\mu$ l of Lipofectamine  
487 RNAiMax and different miRNAs for a final concentration of 10nM and plated in 12-well  
488 plates. miRNA transfection efficiency in different cell lines was confirmed using siGlo Red  
489 Transfection Indicator (Horizon, D-001630-02-05).

### 490 **Confirmation assay**

491 HeLa cells were reverse transfected with 10 nM of the indicated miRNAs using  
492 Lipofectamine RNAiMAX according to manufacturer's instructions. 72h after transfection



493 the cells were trypsinized, harvested in 1X flow cytometry buffer (1X PBS, 1mM EDTA, 2%  
494 FBS) and analyzed for green and red fluorescence by flow cytometry using a BD  
495 FACSymphony instrument (BD-Biosciences).

## 496 **Western blots and antibodies**

497 After incubation for 72h, transfected cells were washed once with 1X PBS, lysed directly in  
498 wells with 100-150 $\mu$ l of SDS Lysis buffer (62.5mM Tris-Cl, pH 6.8, 2% SDS) and sonicated  
499 (amplitude of 35%; 10 pulses with 2 seconds ON and 0.5 seconds OFF). The lysates were  
500 centrifuged for 2 minutes and protein concentrations quantitated by BCA Protein Assay  
501 (Pierce). Lysates (10  $\mu$ g of protein/well) were run on 20-well 10-20% NuPage BisTris midi  
502 gels in 1X MES buffer (ThermoFisher Scientific) and transferred to polyvinylidene  
503 difluoride (PVDF) membranes using 25 mM Tris-HCl pH 7.6, 192 mM glycine, and 10%  
504 methanol. Membranes were blocked in 5% nonfat dried milk in Tris-buffered saline [pH  
505 7.4], 0.05% Tween 20 (TBST) and then incubated with primary antibodies as follows:  
506 mouse monoclonal anti-E6AP (clone E4) at 1:1000 dilution (sc-166689 from Santa Cruz  
507 Biotechnology); rabbit monoclonal anti-cleaved PARP (Asp214) (D64E10 XP® #5625 from  
508 Cell Signaling Technologies); mouse monoclonal anti-HPV18-E6 (clone G-7) at a 1:250  
509 dilution (sc-365089 from Santa Cruz Biotechnology); and mouse monoclonal anti-HPV18-  
510 E7 (clone F-7) at a 1:250 dilution (sc-365035 from Santa Cruz Biotechnology). Membranes  
511 were washed in TBST and incubated with horseradish peroxidase (HRP)-conjugated anti-  
512 mouse antibody at a 1:1,000 dilution (R1005 from Kindle Biosciences). The primary  
513 antibodies against  $\beta$ -Actin and P53 were directly conjugated to HRP and were used as  
514 follows: mouse monoclonal anti- $\beta$ -Actin-HRP at a 1:50,000 dilution (A3854 from Millipore  
515 Sigma); and goat polyclonal anti-p53-HRP at a 1:3,000 dilution (HAF1355 from R&D

516 systems). All blots were developed using KwikQuant Ultra Digital-ECL™ Substrate Solution  
517 and processed using KwikQuant™ Imager (Kindle Bioscience LLC). Western blots were  
518 quantified using the Image Studio Lite program (LI-COR Biotechnologies).

## 519 **RNA isolation and qRT-PCR.**

520 At 72h post-transfection, total RNA was isolated using the Nucleospin RNA kit (Takara Bio)  
521 according to the manufacturer's instructions. Samples were quantified using NanoDrop™  
522 Lite Spectrophotometer and equal amounts of RNA (500ng) were reverse transcribed using  
523 the high-capacity cDNA reverse transcription kit (Applied Biosystems). Quantitative real-  
524 time PCR (qRT-PCR) was performed in an Applied Biosystems ABI 7500 fast sequence  
525 detection system using TaqMan Fast Advanced Master Mix (ThermoFisher Scientific), and  
526 the following TaqMan custom gene expression assays for HPV18-E6E7: HPV18-E6E7 FWD  
527 5'-CAACCGAGCACGACAGGAA-3'; HPV18-E6E7 PROBE 5'-  
528 AATATTAAGTATGCATGGACCTAAGGCAACATTGCAA-3'; and HPV18-E6E7 REV 5'-  
529 CTCGTCGGGCTGGTAAATGTT-3' and for HPV16-E6E7: HPV16-E6-FWD 5'-  
530 AGGAGCGACCCGGAAAGT-3'; HPV16-E6-PROBE 5'-  
531 ACCACAGTTATGCACAGAGCTGCAAACAA-3'; and HPV16-E6-REV 5'-  
532 CACGTCGCAGTAACTGTTGCTT-3'. All reactions were normalized using a TaqMan gene  
533 expression assay for PPIA (Hs99999904\_m1 ThermoFisher Scientific).

## 534 **Luciferase assays**

535 C33A cells were transfected in 12-well plates with 10 nM of miRNAs as described above.  
536 After 24h, the miRNA transfection mix was removed and cells were transfected with 0.5 µg  
537 of either plasmid pGL4-LCRHPV16 (p6239, HPV16 nt 7000-85) [55] or pGL4-LCRHPV18

538 (p5194, HPV18 nt 6943-105) [57], containing the firefly luciferase ORF under the control of  
539 the HPV16 and HPV18 LCRs respectively, together with 0.5 $\mu$ g of a plasmid expressing the  
540 renilla luciferase under the control of the human  $\beta$ -actin promoter using Lipofectamine  
541 3000 (ThermoFisher Scientific) according to manufacturer's protocol. At 48h post-  
542 transfection of plasmids (72 hours after miRNA transfection), cells were lysed in the plate  
543 with 250  $\mu$ l of 1x Passive Lysis Buffer and luciferase activity was determined using the  
544 Dual-Luciferase Reporter Assay System (Promega) according to the manufacturer's  
545 instructions. Luciferase intensities were measured using a SpectraMax L luminescence  
546 microplate reader (Molecular Devices). Firefly luciferase readings were normalized to the  
547 respective renilla luciferase readings.

## 548 **Apoptosis assays**

549 HeLa cells were reverse transfected with 10 nM of the different miRNAs either alone or  
550 combined with 20 nM of siRNAs directed to p53 (Dharmacon, D-003329-26: 5'-  
551 GCUUCGAGAUGUCCGAGA-3') or its C911 version (sense, 5'-GCUUCGAGUACUCCGAGA-  
552 UU-3') using Lipofectamine RNAiMAX according to manufacturer's instructions. After  
553 incubation for 72h, attached cells were trypsinized and combined with all non-adherent  
554 cells in the supernatant and PBS washes. The cells were stained with Annexin V using the  
555 Dead Cell Apoptosis Kit with Annexin V Alexa Fluor™ 488 & Propidium Iodide (PI)  
556 (ThermoFisher Scientific #V13241 and #V13245). Stained cells were analyzed by flow  
557 cytometry using a BD FACSCanto flow cytometer (BD Biosciences).

## 558 **Figures and statistics**

559 All graphics and statistical analyses were conducted using Prism 8 (GraphPad). When the  
560 values corresponding to mock transfections were used to normalize other values obtained  
561 in an experiment, the mock values were not included in the corresponding graphic since  
562 invariably their mean is equal to one and their standard deviation is zero. Figures were  
563 assembled using Affinity Photo (Affinity).

## 564 **Acknowledgements**

565 We thank other members of the Howley laboratory for helpful discussions and suggestions.  
566 All plasmids generated in the Howley laboratory that are described in this manuscript are  
567 available through Addgene. This work has been supported by NIH grant R35CA197262 to  
568 P.M.H.

## 570 **Bibliography**

- 571 1. Howley PM, Schiller JT, Lowy DR. Papillomaviruses. In: Knipe DM, Howley PM,  
572 editors. Fields Virology. 6th ed. Philadelphia: Lippincott, Williams and Wilkins; 2013. p.  
573 1662-703.
- 574 2. de Martel C, Plummer M, Vignat J, Franceschi S. Worldwide burden of cancer  
575 attributable to HPV by site, country and HPV type. Int J Cancer. 2017;141(4):664-70. Epub  
576 2017/04/04. doi: 10.1002/ijc.30716. PubMed PMID: 28369882; PubMed Central PMCID:  
577 PMC5520228.
- 578 3. Goodwin EC, DiMaio D. Repression of human papillomavirus oncogenes in HeLa  
579 cervical carcinoma cells causes the orderly reactivation of dormant tumor suppressor

- 580 pathways. Proc Natl Acad Sci U S A. 2000;97(23):12513-8. Epub 2000/11/09. doi:  
581 10.1073/pnas.97.23.12513. PubMed PMID: 11070078; PubMed Central PMCID:  
582 PMCPMC18795.
- 583 4. Wells SI, Francis DA, Karpova AY, Dowhanick JJ, Benson JD, Howley PM.  
584 Papillomavirus E2 induces senescence in HPV positive cells via pRB- and p21<sup>CIP</sup>-dependent  
585 pathways. EMBO J. 2000;19:5762-71.
- 586 5. Scheffner M, Werness BA, Huibregtse JM, Levine AJ, Howley PM. The E6 oncoprotein  
587 encoded by human papillomavirus types 16 and 18 promotes the degradation of p53. Cell.  
588 1990;63(6):1129-36. Epub 1990/12/21. doi: 10.1016/0092-8674(90)90409-8. PubMed  
589 PMID: 2175676.
- 590 6. Huibregtse JM, Scheffner M, Howley PM. Cloning and expression of the cDNA for E6-  
591 AP: A protein that mediates the interaction of the human papillomavirus E6 oncoprotein  
592 with p53. Mol Cell Biol. 1993;13:775-84.
- 593 7. Huibregtse JM, Scheffner M, Howley PM. Localization of the E6-AP regions that  
594 direct HPV E6 binding, association with p53, and ubiquitination of associated proteins. Mol  
595 Cell Biol. 1993;13:4918-27.
- 596 8. Scheffner M, Huibregtse JM, Vierstra RD, Howley PM. The HPV-16 E6 and E6-AP  
597 complex functions as a ubiquitin-protein ligase in the ubiquitination of p53. Cell.  
598 1993;75:495-505.
- 599 9. Park RB, Androphy EJ. Genetic analysis of high-risk e6 in episomal maintenance of  
600 human papillomavirus genomes in primary human keratinocytes. J Virol.  
601 2002;76(22):11359-64. PubMed PMID: 12388696.

- 602 10. Butz K, Ristriani T, Hengstermann A, Denk C, Scheffner M, Hoppe-Seyler F. siRNA  
603 targeting of the viral E6 oncogene efficiently kills human papillomavirus-positive cancer  
604 cells. *Oncogene*. 2003;22:5938-3945. doi: [10.1038/sj.onc.1206894](https://doi.org/10.1038/sj.onc.1206894)  
605 [1206894](#) [pii]. PubMed PMID: 12955072.
- 606 11. Chirayil R, Kincaid RP, Dahlke C, Kuny CV, Dalken N, Spohn M, et al. Identification of  
607 virus-encoded microRNAs in divergent Papillomaviruses. *PLoS Pathog*.  
608 2018;14(7):e1007156. Epub 2018/07/27. doi: [10.1371/journal.ppat.1007156](https://doi.org/10.1371/journal.ppat.1007156). PubMed  
609 PMID: 30048533; PubMed Central PMCID: PMC6062147.
- 610 12. Wald AI, Hoskins EE, Wells SI, Ferris RL, Khan SA. Alteration of microRNA profiles in  
611 squamous cell carcinoma of the head and neck cell lines by human papillomavirus. *Head*  
612 *Neck*. 2011;33(4):504-12. Epub 2010/07/24. doi: [10.1002/hed.21475](https://doi.org/10.1002/hed.21475). PubMed PMID:  
613 20652977; PubMed Central PMCID: PMC3080748.
- 614 13. Wang X, Wang HK, Li Y, Hafner M, Banerjee NS, Tang S, et al. microRNAs are  
615 biomarkers of oncogenic human papillomavirus infections. *Proc Natl Acad Sci U S A*.  
616 2014;111(11):4262-7. Epub 2014/03/05. doi: [10.1073/pnas.1401430111](https://doi.org/10.1073/pnas.1401430111). PubMed PMID:  
617 24591631; PubMed Central PMCID: PMC3964092.
- 618 14. Tornesello ML, Faraonio R, Buonaguro L, Annunziata C, Starita N, Cerasuolo A, et al.  
619 The Role of microRNAs, Long Non-coding RNAs, and Circular RNAs in Cervical Cancer.  
620 *Front Oncol*. 2020;10:150. Epub 2020/03/11. doi: [10.3389/fonc.2020.00150](https://doi.org/10.3389/fonc.2020.00150). PubMed  
621 PMID: 32154165; PubMed Central PMCID: PMC7044410.
- 622 15. Scheffner M, Takahashi T, Huibregtse JM, Minna JD, Howley PM. Interaction of the  
623 human papillomavirus type 16 E6 oncoprotein with wild-type and mutant human p53

- 624 proteins. *J Virol.* 1992;66(8):5100-5. Epub 1992/08/01. PubMed PMID: 1321290; PubMed  
625 Central PMCID: PMCPMC241378.
- 626 16. Hubbert NL, Sedman SA, Schiller JT. Human papillomavirus type 16 E6 increases the  
627 degradation rate of p53 in human keratinocytes. *Journal of virology.* 1992;66(10):6237-41.  
628 PubMed PMID: 1326671.
- 629 17. Jung HM, Phillips BL, Chan EK. miR-375 activates p21 and suppresses telomerase  
630 activity by coordinately regulating HPV E6/E7, E6AP, CIP2A, and 14-3-3zeta. *Mol Cancer.*  
631 2014;13:80. Epub 2014/04/09. doi: 10.1186/1476-4598-13-80. PubMed PMID: 24708873;  
632 PubMed Central PMCID: PMCPMC4021670.
- 633 18. Kuhnle S, Martinez-Noel G, Leclere F, Hayes SD, Harper JW, Howley PM. Angelman  
634 syndrome-associated point mutations in the Zn(2+)-binding N-terminal (AZUL) domain of  
635 UBE3A ubiquitin ligase inhibit binding to the proteasome. *J Biol Chem.*  
636 2018;293(47):18387-99. Epub 2018/09/28. doi: 10.1074/jbc.RA118.004653. PubMed  
637 PMID: 30257870; PubMed Central PMCID: PMCPMC6254356.
- 638 19. Scheffner M, Munger K, Byrne JC, Howley PM. The state of the p53 and  
639 retinoblastoma genes in human cervical carcinoma cell lines. *Proc Natl Acad Sci U S A.*  
640 1991;88(13):5523-7. Epub 1991/07/01. doi: 10.1073/pnas.88.13.5523. PubMed PMID:  
641 1648218; PubMed Central PMCID: PMCPMC51909.
- 642 20. Munger K, Phelps WC, Bubb V, Howley PM, Schlegel R. The E6 and E7 genes of the  
643 human papillomavirus type 16 together are necessary and sufficient for transformation of  
644 primary human keratinocytes. *J Virol.* 1989;63(10):4417-21. Epub 1989/10/01. PubMed  
645 PMID: 2476573; PubMed Central PMCID: PMCPMC251060.

- 646 21. Liu X. Up-regulation of miR-20a by HPV16 E6 exerts growth-promoting effects by  
647 targeting PDCD6 in cervical carcinoma cells. *Biomed Pharmacother.* 2018;102:996-1002.  
648 Epub 2018/05/02. doi: 10.1016/j.biopha.2018.03.154. PubMed PMID: 29710555.
- 649 22. Buehler E, Chen YC, Martin S. C911: A bench-level control for sequence specific  
650 siRNA off-target effects. *PLoS One.* 2012;7(12):e51942. Epub 2012/12/20. doi:  
651 10.1371/journal.pone.0051942. PubMed PMID: 23251657; PubMed Central PMCID:  
652 PMCPMC3522603.
- 653 23. Jiang Y, Hou R, Li S, Li S, Dang G. MicroRNA-302 inhibits cell migration and invasion  
654 in cervical cancer by targeting DCUN1D1. *Exp Ther Med.* 2018;16(2):1000-8. Epub  
655 2018/08/18. doi: 10.3892/etm.2018.6223. PubMed PMID: 30116351; PubMed Central  
656 PMCID: PMCPMC6090382.
- 657 24. Li GC, Cao XY, Li YN, Qiu YY, Li YN, Liu XJ, et al. MicroRNA-374b inhibits cervical  
658 cancer cell proliferation and induces apoptosis through the p38/ERK signaling pathway by  
659 binding to JAM-2. *J Cell Physiol.* 2018;233(9):7379-90. Epub 2018/03/27. doi:  
660 10.1002/jcp.26574. PubMed PMID: 29575013.
- 661 25. Mou Z, Xu X, Dong M, Xu J. MicroRNA-148b Acts as a Tumor Suppressor in Cervical  
662 Cancer by Inducing G1/S-Phase Cell Cycle Arrest and Apoptosis in a Caspase-3-Dependent  
663 Manner. *Med Sci Monit.* 2016;22:2809-15. Epub 2016/08/10. doi: 10.12659/msm.896862.  
664 PubMed PMID: 27505047; PubMed Central PMCID: PMCPMC4982527.
- 665 26. Ji F, Du R, Chen T, Zhang M, Zhu Y, Luo X, et al. Circular RNA circSLC26A4  
666 Accelerates Cervical Cancer Progression via miR-1287-5p/HOXA7 Axis. *Mol Ther Nucleic  
667 Acids.* 2020;19:413-20. Epub 2020/01/03. doi: 10.1016/j.omtn.2019.11.032. PubMed  
668 PMID: 31896069; PubMed Central PMCID: PMCPMC6940609.



- 669 27. Abdelmohsen K, Kim MM, Srikantan S, Mercken EM, Brennan SE, Wilson GM, et al.  
670 miR-519 suppresses tumor growth by reducing HuR levels. *Cell Cycle*. 2010;9(7):1354-9.  
671 Epub 2010/03/23. doi: 10.4161/cc.9.7.11164. PubMed PMID: 20305372; PubMed Central  
672 PMCID: PMCPMC3057889.
- 673 28. Abdelmohsen K, Srikantan S, Tominaga K, Kang MJ, Yaniv Y, Martindale JL, et al.  
674 Growth inhibition by miR-519 via multiple p21-inducing pathways. *Mol Cell Biol*.  
675 2012;32(13):2530-48. Epub 2012/05/02. doi: 10.1128/mcb.00510-12. PubMed PMID:  
676 22547681; PubMed Central PMCID: PMCPMC3434494.
- 677 29. Chen Y, Wang X. miRDB: an online database for prediction of functional microRNA  
678 targets. *Nucleic Acids Res*. 2020;48(D1):D127-D31. Epub 2019/09/11. doi:  
679 10.1093/nar/gkz757. PubMed PMID: 31504780; PubMed Central PMCID:  
680 PMCPMC6943051.
- 681 30. Liu W, Wang X. Prediction of functional microRNA targets by integrative modeling of  
682 microRNA binding and target expression data. *Genome Biol*. 2019;20(1):18. Epub  
683 2019/01/24. doi: 10.1186/s13059-019-1629-z. PubMed PMID: 30670076; PubMed  
684 Central PMCID: PMCPMC6341724.
- 685 31. Kim JY, Kim KM, Yang JH, Cho SS, Kim SJ, Park SJ, et al. Induction of E6AP by  
686 microRNA-302c dysregulation inhibits TGF-beta-dependent fibrogenesis in hepatic stellate  
687 cells. *Sci Rep*. 2020;10(1):444. Epub 2020/01/18. doi: 10.1038/s41598-019-57322-w.  
688 PubMed PMID: 31949242; PubMed Central PMCID: PMCPMC6965100.
- 689 32. Kedde M, Strasser MJ, Boldajipour B, Oude Vrielink JA, Slanchev K, le Sage C, et al.  
690 RNA-binding protein Dnd1 inhibits microRNA access to target mRNA. *Cell*.

691 2007;131(7):1273-86. Epub 2007/12/25. doi: 10.1016/j.cell.2007.11.034. PubMed PMID:  
692 18155131.

693 33. Mockly S, Seitz H. Inconsistencies and Limitations of Current MicroRNA Target  
694 Identification Methods. *Methods Mol Biol.* 2019;1970:291-314. Epub 2019/04/10. doi:  
695 10.1007/978-1-4939-9207-2\_16. PubMed PMID: 30963499.

696 34. Girardi E, Lopez P, Pfeffer S. On the Importance of Host MicroRNAs During Viral  
697 Infection. *Front Genet.* 2018;9:439. Epub 2018/10/20. doi: 10.3389/fgene.2018.00439.  
698 PubMed PMID: 30333857; PubMed Central PMCID: PMC6176045.

699 35. Wang F, Li Y, Zhou J, Xu J, Peng C, Ye F, et al. miR-375 is down-regulated in  
700 squamous cervical cancer and inhibits cell migration and invasion via targeting  
701 transcription factor SP1. *Am J Pathol.* 2011;179(5):2580-8. Epub 2011/09/29. doi:  
702 10.1016/j.ajpath.2011.07.037. PubMed PMID: 21945323; PubMed Central PMCID:  
703 PMC3204087.

704 36. Hoppe-Seyler F, Butz K. Activation of human papillomavirus type 18 E6-E7  
705 oncogene expression by transcription factor Sp1. *Nucleic Acids Res.* 1992;20(24):6701-6.  
706 Epub 1992/12/25. doi: 10.1093/nar/20.24.6701. PubMed PMID: 1336181; PubMed  
707 Central PMCID: PMC334589.

708 37. Tan SH, Leong LE, Walker PA, Bernard HU. The human papillomavirus type 16 E2  
709 transcription factor binds with low cooperativity to two flanking sites and represses the E6  
710 promoter through displacement of Sp1 and TFIID. *J Virol.* 1994;68(10):6411-20. Epub  
711 1994/10/01. PubMed PMID: 8083979; PubMed Central PMCID: PMC237061.

712 38. Hong L, Ya-Wei L, Hai W, Qiang Z, Jun-Jie L, Huang A, et al. MiR-519a functions as a  
713 tumor suppressor in glioma by targeting the oncogenic STAT3 pathway. *J Neurooncol.*

- 714 2016;128(1):35-45. Epub 2016/03/14. doi: 10.1007/s11060-016-2095-z. PubMed PMID:  
715 26970980.
- 716 39. Deng X, Zhao Y, Wang B. miR-519d-mediated downregulation of STAT3 suppresses  
717 breast cancer progression. *Oncol Rep.* 2015;34(4):2188-94. Epub 2015/08/05. doi:  
718 10.3892/or.2015.4160. PubMed PMID: 26238950.
- 719 40. Morgan EL, Wasson CW, Hanson L, Kealy D, Pentland I, McGuire V, et al. STAT3  
720 activation by E6 is essential for the differentiation-dependent HPV18 life cycle. *PLoS*  
721 *Pathog.* 2018;14(4):e1006975. Epub 2018/04/10. doi: 10.1371/journal.ppat.1006975.  
722 PubMed PMID: 29630659; PubMed Central PMCID: PMC5908086.
- 723 41. Shukla S, Mahata S, Shishodia G, Pandey A, Tyagi A, Vishnoi K, et al. Functional  
724 regulatory role of STAT3 in HPV16-mediated cervical carcinogenesis. *PLoS One.*  
725 2013;8(7):e67849. Epub 2013/07/23. doi: 10.1371/journal.pone.0067849. PubMed PMID:  
726 23874455; PubMed Central PMCID: PMC3715508.
- 727 42. Xun Y, Tang Y, Hu L, Xiao H, Long S, Gong M, et al. Purification and Identification of  
728 miRNA Target Sites in Genome Using DNA Affinity Precipitation. *Front Genet.* 2019;10:778.  
729 Epub 2019/10/02. doi: 10.3389/fgene.2019.00778. PubMed PMID: 31572429; PubMed  
730 Central PMCID: PMC6751328.
- 731 43. Kracikova M, Akiri G, George A, Sachidanandam R, Aaronson SA. A threshold  
732 mechanism mediates p53 cell fate decision between growth arrest and apoptosis. *Cell*  
733 *Death Differ.* 2013;20(4):576-88. Epub 2013/01/12. doi: 10.1038/cdd.2012.155. PubMed  
734 PMID: 23306555; PubMed Central PMCID: PMC3595483.

- 735 44. Bartel DP. MicroRNAs: target recognition and regulatory functions. Cell.  
736 2009;136(2):215-33. Epub 2009/01/27. doi: 10.1016/j.cell.2009.01.002. PubMed PMID:  
737 19167326; PubMed Central PMCID: PMCPMC3794896.
- 738 45. Shukla GC, Singh J, Barik S. MicroRNAs: Processing, Maturation, Target Recognition  
739 and Regulatory Functions. Mol Cell Pharmacol. 2011;3(3):83-92. Epub 2011/01/01.  
740 PubMed PMID: 22468167; PubMed Central PMCID: PMCPMC3315687.
- 741 46. Broughton JP, Lovci MT, Huang JL, Yeo GW, Pasquinelli AE. Pairing beyond the Seed  
742 Supports MicroRNA Targeting Specificity. Mol Cell. 2016;64(2):320-33. Epub 2016/10/22.  
743 doi: 10.1016/j.molcel.2016.09.004. PubMed PMID: 27720646; PubMed Central PMCID:  
744 PMCPMC5074850.
- 745 47. Lee RC, Feinbaum RL, Ambros V. The *C. elegans* heterochronic gene *lin-4* encodes  
746 small RNAs with antisense complementarity to *lin-14*. Cell. 1993;75(5):843-54. Epub  
747 1993/12/03. doi: 10.1016/0092-8674(93)90529-y. PubMed PMID: 8252621.
- 748 48. Wightman B, Ha I, Ruvkun G. Posttranscriptional regulation of the heterochronic  
749 gene *lin-14* by *lin-4* mediates temporal pattern formation in *C. elegans*. Cell.  
750 1993;75(5):855-62. Epub 1993/12/03. doi: 10.1016/0092-8674(93)90530-4. PubMed  
751 PMID: 8252622.
- 752 49. Bonneau E, Neveu B, Kostantin E, Tsongalis GJ, De Guire V. How close are miRNAs  
753 from clinical practice? A perspective on the diagnostic and therapeutic market. Ejifcc.  
754 2019;30(2):114-27. Epub 2019/07/03. PubMed PMID: 31263388; PubMed Central PMCID:  
755 PMCPMC6599191.
- 756 50. Hanna J, Hossain GS, Kocerha J. The Potential for microRNA Therapeutics and  
757 Clinical Research. Front Genet. 2019;10:478. Epub 2019/06/04. doi:

- 758 10.3389/fgene.2019.00478. PubMed PMID: 31156715; PubMed Central PMCID:  
759 PMCPMC6532434.
- 760 51. Emanuele MJ, Elia AE, Xu Q, Thoma CR, Izhar L, Leng Y, et al. Global identification of  
761 modular cullin-RING ligase substrates. *Cell*. 2011;147(2):459-74. Epub 2011/10/04. doi:  
762 10.1016/j.cell.2011.09.019. PubMed PMID: 21963094; PubMed Central PMCID:  
763 PMCPMC3226719.
- 764 52. Lin HC, Yeh CW, Chen YF, Lee TT, Hsieh PY, Rusnac DV, et al. C-Terminal End-  
765 Directed Protein Elimination by CRL2 Ubiquitin Ligases. *Mol Cell*. 2018;70(4):602-13 e3.  
766 Epub 2018/05/19. doi: 10.1016/j.molcel.2018.04.006. PubMed PMID: 29775578; PubMed  
767 Central PMCID: PMCPMC6145449.
- 768 53. Yen HC, Elledge SJ. Identification of SCF ubiquitin ligase substrates by global protein  
769 stability profiling. *Science*. 2008;322(5903):923-9. Epub 2008/11/08. doi:  
770 10.1126/science.1160462. PubMed PMID: 18988848.
- 771 54. Yen HC, Xu Q, Chou DM, Zhao Z, Elledge SJ. Global protein stability profiling in  
772 mammalian cells. *Science*. 2008;322(5903):918-23. Epub 2008/11/08. doi:  
773 10.1126/science.1160489. PubMed PMID: 18988847.
- 774 55. Ottinger M, Smith JA, Schweiger MR, Robbins D, Powell ML, You J, et al. Cell-type  
775 specific transcriptional activities among different papillomavirus long control regions and  
776 their regulation by E2. *Virology*. 2009;395(2):161-71. Epub 2009/10/20. doi:  
777 10.1016/j.virol.2009.09.027. PubMed PMID: 19836046; PubMed Central PMCID:  
778 PMCPMC2787971.
- 779 56. Zhang JH, Chung TD, Oldenburg KR. A Simple Statistical Parameter for Use in  
780 Evaluation and Validation of High Throughput Screening Assays. *J Biomol Screen*.

781 1999;4(2):67-73. Epub 2000/06/06. doi: 10.1177/108705719900400206. PubMed PMID:  
782 10838414.

783 57. Schweiger MR, Ottinger M, You J, Howley PM. Brd4-independent transcriptional  
784 repression function of the papillomavirus e2 proteins. J Virol. 2007;81(18):9612-22. Epub  
785 2007/07/13. doi: 10.1128/jvi.00447-07. PubMed PMID: 17626100; PubMed Central  
786 PMCID: PMCPMC2045424.

787

## 788 **Figure captions**

789

### 790 **Fig 1. Schematic representation of reporter cassettes.**

791 **A.** Reporter cassette of pHAGE-P CMVt RIG p53(R273C). **B.** Reporter cassette in pHAGE-P  
792 CMVt RIG3 p53(R273C). CMVp: CMV promoter, IRES: Encephalomyocarditis virus internal  
793 ribosomal entry site, H2B: histone 2B (H2BC11), SG linker: serine-glycine linker.

794

### 795 **Fig 2. Effect of miRNAs transfection on p53, E6AP, and E6 protein levels in HeLa cells.**

796 Cells were lysed 72 h post-transfection and the lysates were resolved by SDS-PAGE. Protein  
797 levels of p53, E6AP, E6, and actin were visualized by western blotting. **A, C, and E.** Western  
798 blot results from a single experiment. **B, D, and F.** Quantification of p53 from western blot  
799 experiments. Values obtained for p53 were normalized to the amount of actin in the same  
800 sample and then all values were divided by the corresponding value obtained with the  
801 mock transfection in the same blot. Circles represent values from independent experiments

802 and the bars show the mean  $\pm$  standard deviation. To determine significant differences  
803 between the samples in an experiment we used the "one-way ANOVA" test (A.  $F(16,$   
804  $34)=8.271$   $p<0.0001$ ,  $n=3$ ; B.  $F(14, 30)=17.76$   $p<0.0001$ ,  $n=3$ ; C.  $F(3, 12)=52.63$   $p<0.0001$ ,  
805  $n=4$ ). We then compared each sample with the cells transfected with the Ctrl.1 miRNA  
806 using the "Dunnett's multiple comparisons test" (\* =  $p<0.01$ ).

807

808 **Fig 3. Effect of transfection of selected miRNAs on p53 and E6AP protein levels in**  
809 **different cell lines.**

810 72 h after transfection cells were lysed and the protein extracts were resolved by SDS-  
811 PAGE, and the p53, E6AP, and actin proteins levels were determined by western blotting.

812

813 **Fig 4. Effect of selected miRNAs on HPV E6 and E7 expression.**

814 Cells were harvested 72 h post-transfection and then used for the following experiments. **A.**  
815 Western blot showing the effect of the selected miRNAs on E6, E7, and actin protein levels  
816 in HeLa cells. **B.** Effect of ectopic expression of selected miRNAs on the promoter activity of  
817 the HPV16 and HPV18 LCRs using a luciferase reporter assay in C33A cells. Values from  
818 each experiment were normalized to the value obtained for the corresponding mock  
819 transfection. Differences between samples were analyzed by the "one-way ANOVA" test  
820 (HPV 16  $F(12, 38) = 34.91$ ,  $n=4$ ; HPV18  $F(12, 39) = 23.47$   $p<0.0001$ ,  $n=4$ ), then each sample  
821 was compared to the non-treated cells using the "Dunnett's multiple comparisons test" (\* =  
822  $p<0.01$ ). **C.** Expression of the E6/E7 mRNAs after transfection of the selected miRNAs was  
823 quantitated by QRT-PCR. Measures from each experiment were normalized to the value of  
824 the corresponding mock transfection. The same statistical analysis described in B. was

825 applied to these samples (SiHa  $F(12, 26) = 41.38$   $p < 0.0001$ ,  $n=3$ ; HeLa  $F(12, 39) = 42.32$   
826  $p < 0.0001$ ,  $n=4$ ). In B. and C. Circles represent values from independent experiments and  
827 the bars show the mean  $\pm$  standard deviation.

828

829 **Fig 5. Ectopic miRNA expression induces apoptosis in HeLa cells.**

830 Cells were harvested 72 h post-transfection and stained with Annexin V as an indicator of  
831 apoptosis. The percentage of cells stained with Annexin V was determined by flow  
832 cytometry. Variability between samples was first analyzed with the one-way ANOVA test  
833 ( $F(12,26)=48.04$   $p < 0.0001$ ,  $n=3$ ). Then each sample was compared to the non-treated cells  
834 with the "Dunnett's multiple comparisons test" (\* =  $p < 0.01$ ). Circles represent values from  
835 independent experiments and the bars show the mean  $\pm$  standard deviation.

836

837 **Fig 6. Apoptotic effect of the selected miRNAs when transfected into different cell**  
838 **lines.**

839 Cells were transfected with the indicated miRNAs and 72 h later the cells were harvested  
840 and stained with Annexin V as a marker for apoptosis. The percentage of Annexin V  
841 positive cells was quantitated by flow cytometry. Variability between samples for each cell  
842 line was analyzed with the one-way ANOVA test (SiHa  $F(6,21)=45.17$   $p < 0.0001$ ,  $n=4$ ; C33A  
843  $F(6,21)=85.96$   $p < 0.0001$ ,  $n=3$ ; U2OS  $F(6,21)=104.07$   $p < 0.0001$ ,  $n=4$ ). Each sample was then  
844 compared to the non-treated cells with the "Dunnett's multiple comparisons test" (\* =  
845  $p < 0.01$ ). Circles represent values from independent experiments and the bars show the  
846 mean  $\pm$  standard deviation.

847



848 **Fig 7. p53 dependence of apoptotic effect of selected miRNAs in HeLa cells. A.**

849 Cells were transfected with the indicated miRNAs either alone or together with a siRNA  
850 against p53 or its C911 variant. After incubation for 72 h the cells were harvested and  
851 stained with Annexin V as a marker for apoptosis. The percentage of Annexin V stained  
852 cells was determined by flow cytometry. The values obtained for the three transfections  
853 with each miRNA were first analyzed with the one-way ANOVA test (375-3p  $F(2, 6) = 3.075$   
854  $p=0.1204$ ; 498-5p  $F(2, 6) = 1.914$   $p=0.2276$ ; 20a-3p  $F(2, 6) = 0.6553$   $p=0.5528$ ; 148b-5p  
855  $F(2, 6) = 23.57$   $p=0.0014$ ; 374a-3p  $F(2, 6) = 2.681$   $p=0.1472$ ; 519b-3p  $F(2, 6) = 17.71$   
856  $p=0.0030$ ; 1287-5p  $F(2, 6) = 48.00$   $p=0.0002$ ). For all samples  $n=3$ . Then, the values from  
857 samples transfected with the same miRNA were compared with each other using the  
858 "Tukey's multiple comparisons test" (\* =  $p<0.01$ ). **B.** 72 h post-transfection cells were lysed  
859 and the p53, cleaved PARP, and GAPDH proteins levels were determined by SDS-PAGE and  
860 western blotting.

861

862 **Supporting Information**

863

864 **S1 Table. Screen data.**

865

866 **S1 Fig. Alignment of members of the 302/519 family of miRNAs.**

867 Several of the miRNAs identified in our screen have the same seed sequence indicated with  
868 bold letters and underlined. <sup>1</sup> miRNAs with EGFP/DsRed ratios between top 50 positions in  
869 the primary screen.

870

871 **S2 Fig. p53 stabilization in HeLa cells expressing the reporter pHAGE-P CMVt RIG3**

872 **p53(R273C).**

873 72 h after transfection cells were harvested and the percentage of cells expressing mRuby-

874 p53(R273C) was determined by flow cytometry. Columns indicate the means of three

875 independent experiments and the error bars show one standard deviation. Variability

876 between the means was tested using the one-way ANOVA test ( $F(40, 82) = 84.19$

877  $p < 0.0001$ ). Then, each sample was compared to non-treated cells using the "Dunnett's

878 multiple comparisons test" (\* =  $p < 0.01$ ).

879

880 **S3 Fig. Quantification of the effect of miRNAs transfection on E6AP, and E6 protein**

881 **levels in HeLa cells.**

882 Quantification of E6AP and E6 protein levels from western blot experiments. The values for

883 E6AP and E6 were normalized to the amount of actin in the same sample, then all values

884 were divided by the corresponding value of the mock transfection in the same blot. Circles

885 show the values of independent experiments and the bars indicate the mean  $\pm$  standard

886 deviation. The significance of differences between the samples means was determined

887 using the one-way ANOVA test (**A.** E6AP protein levels  $F(16, 34) = 9.540$   $p < 0.0001$ ,  $n = 3$ ; **B.**

888 E6AP protein levels  $F(14, 30) = 1.218$   $p < 0.3135$ ,  $n = 3$ ; **C.** E6AP protein levels  $F(3, 12) = 11.16$

889  $p < 0.0009$ ,  $n = 4$  **D.** E6 protein levels  $F(16, 34) = 8.672$   $p < 0.0001$ ,  $n = 3$ ; **E.** E6 protein levels

890  $F(14, 30) = 18.15$   $p < 0.0001$ ,  $n = 3$ ; **F.** E6 protein levels  $F(3, 12) = 55.35$   $p < 0.0001$ ,  $n = 4$ ). Each

891 sample was then compared to the cells transfected with the Ctrl.1 miRNA using the

892 "Dunnett's multiple comparisons test" (\* =  $p < 0.01$ ).

893

894 **S4 Fig. The protein levels of p53 negatively correlate with those of E6.**

895 The protein levels of p53, E6AP, and E6 calculated from the western blot experiments  
896 displayed in Figs 2 and S3 were used to analyze whether there is a significant correlation  
897 between the levels of these proteins after transfection of HeLa cells with the different  
898 miRNAs. This was done by calculating the Pearson's correlation coefficient ( $r$ ) and a two  
899 tailed p value. **A.** Correlation between E6AP and p53. **B.** Correlation between E6 and p53. **C.**  
900 Correlation between E6AP and E6.

901

902 **S2 Table. List of miRNAs used in this study.**

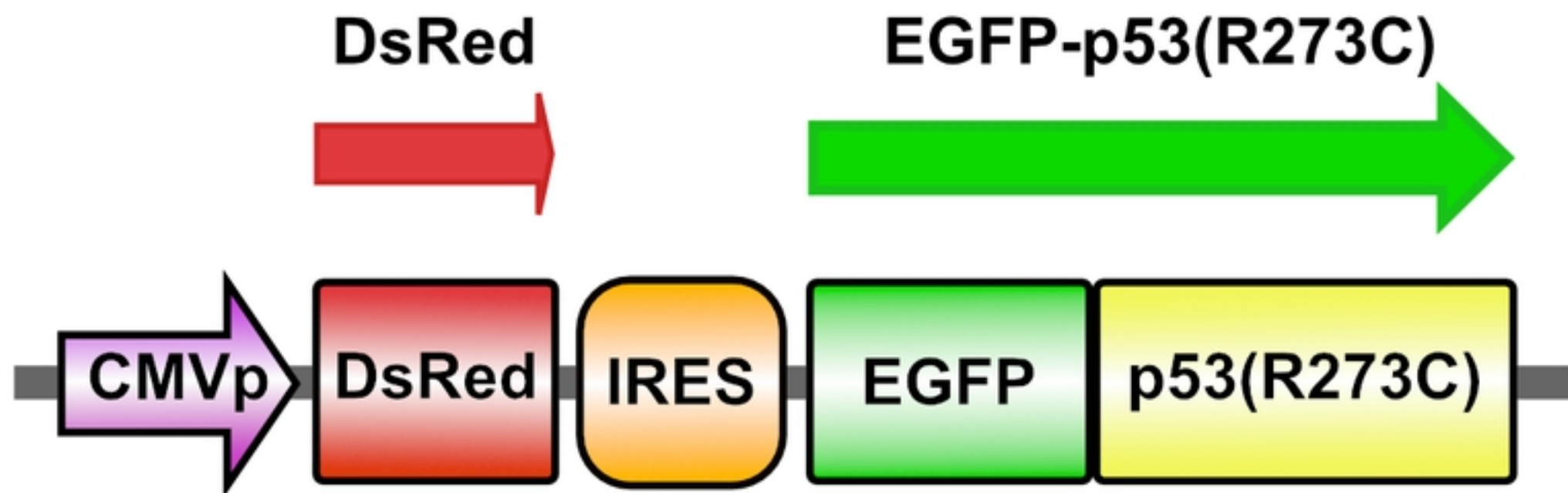
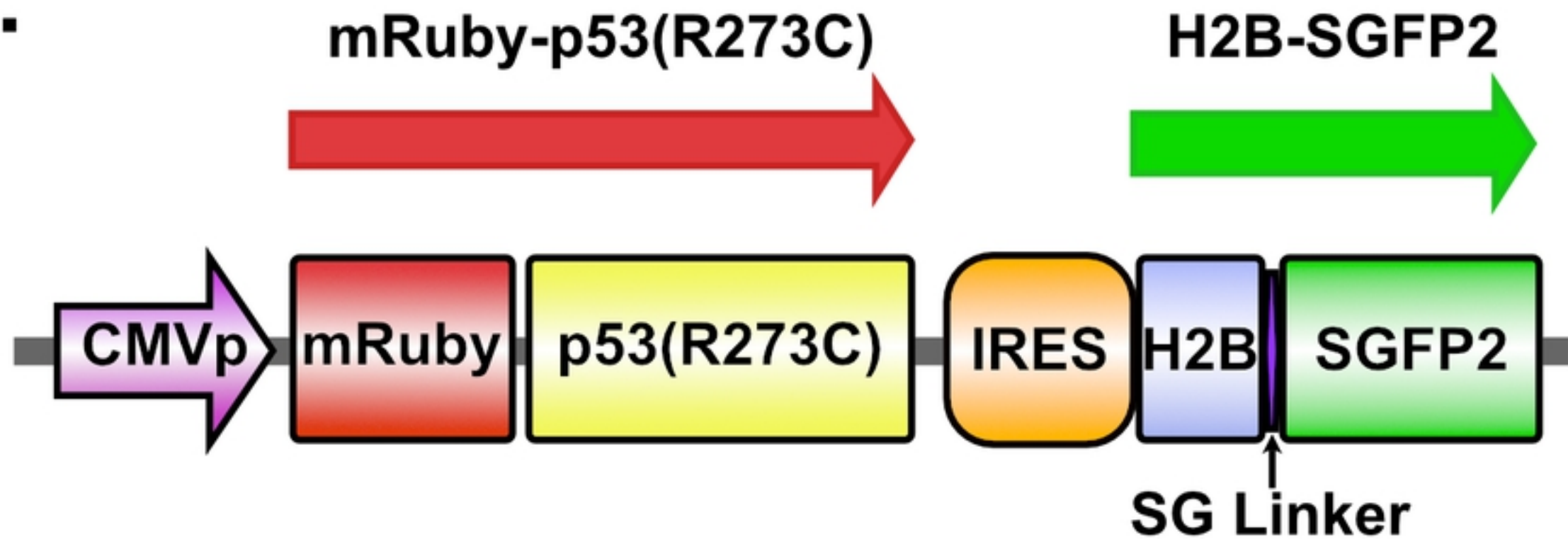
**A.****B.**

Figure 1

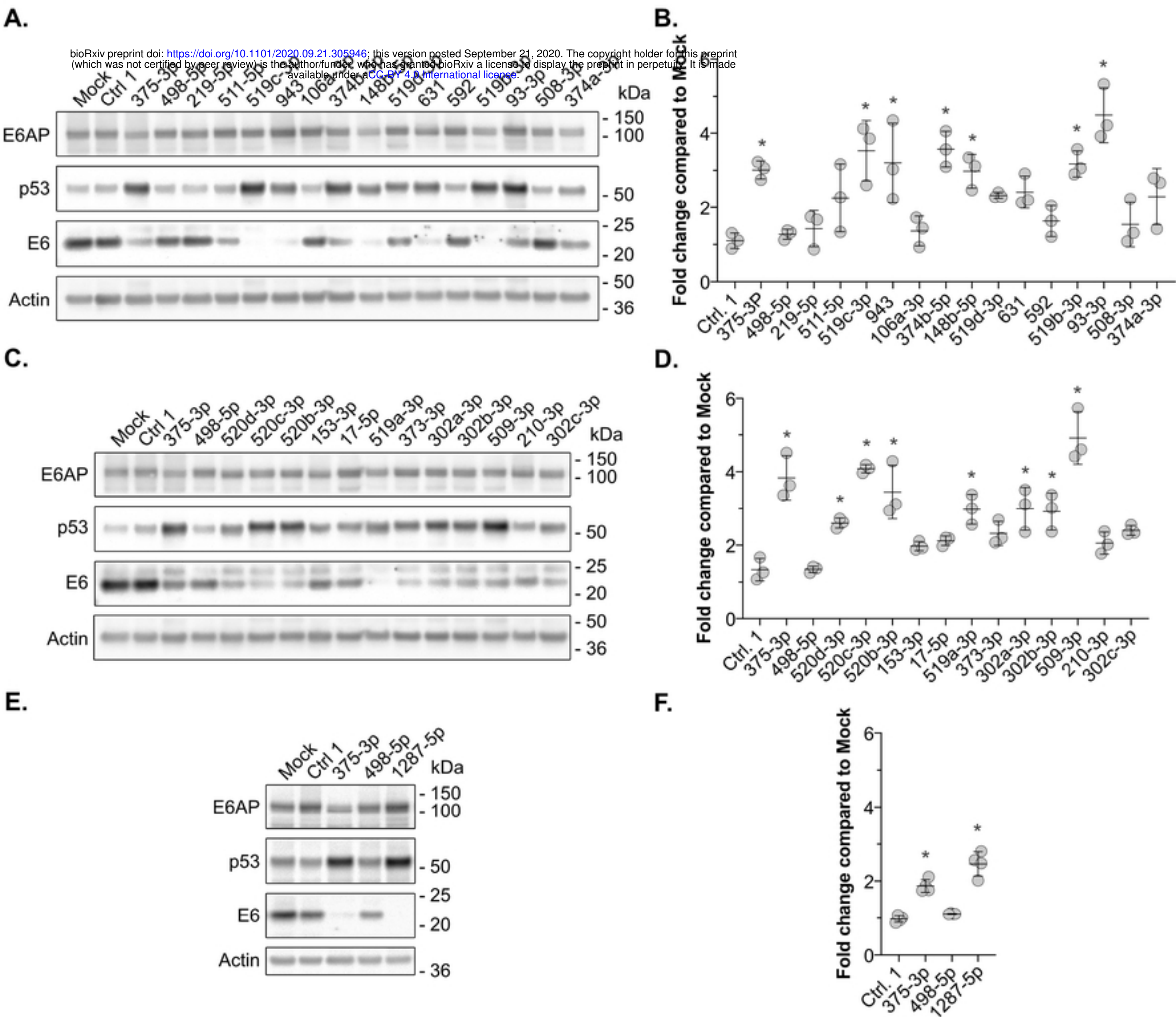


Figure 2

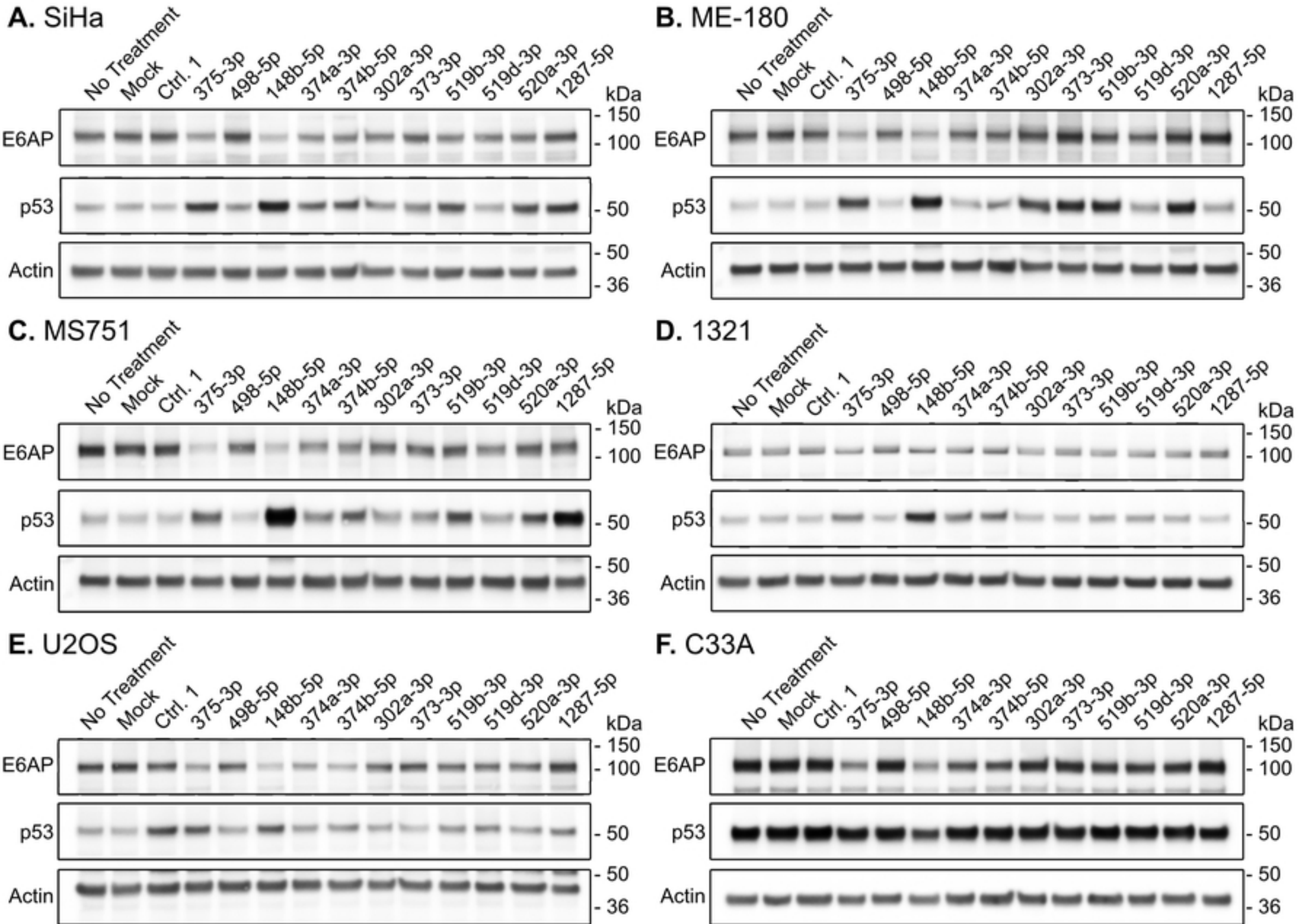


Figure 3

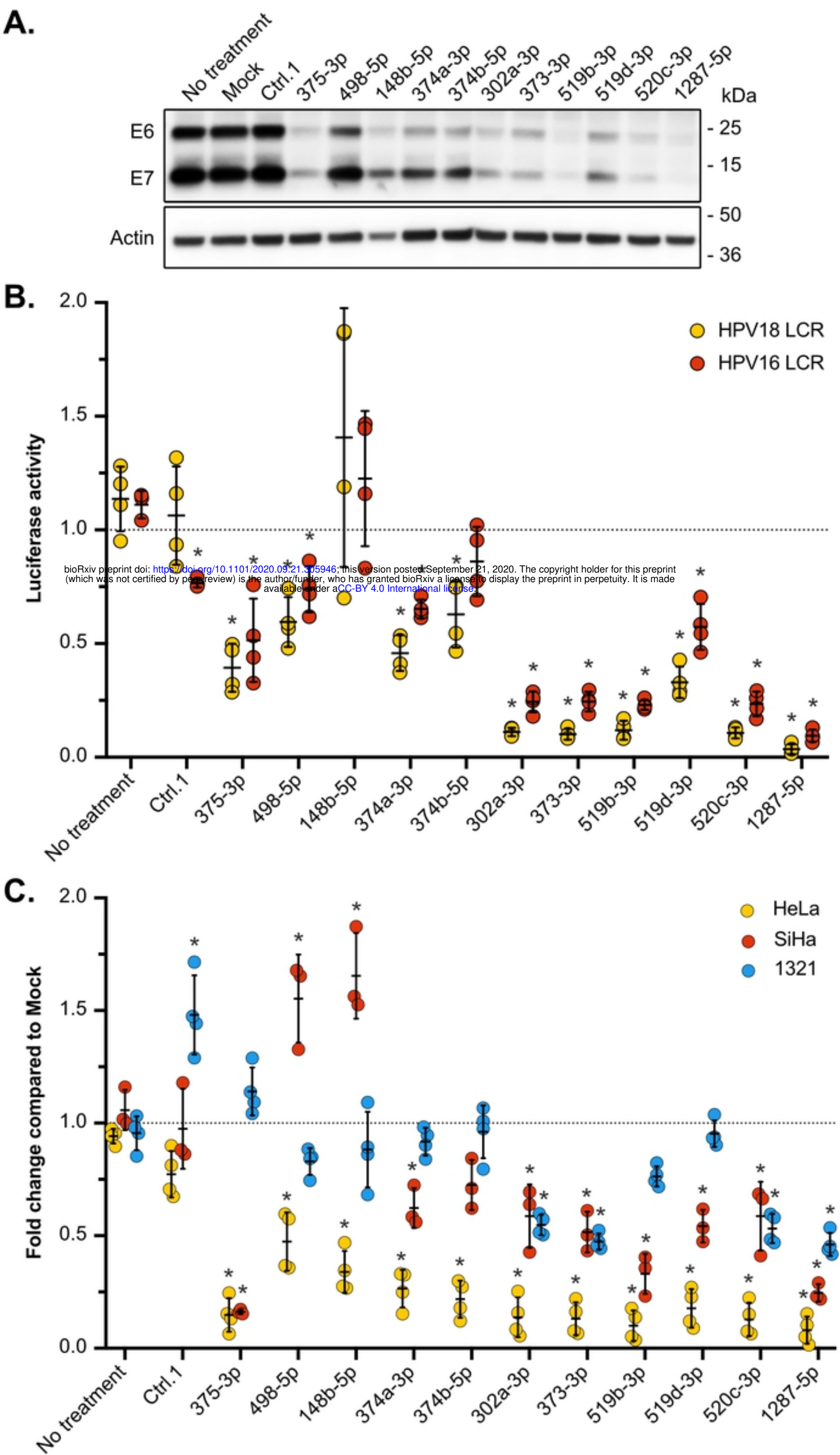


Figure 4

Percentage of Annexin V positive cells

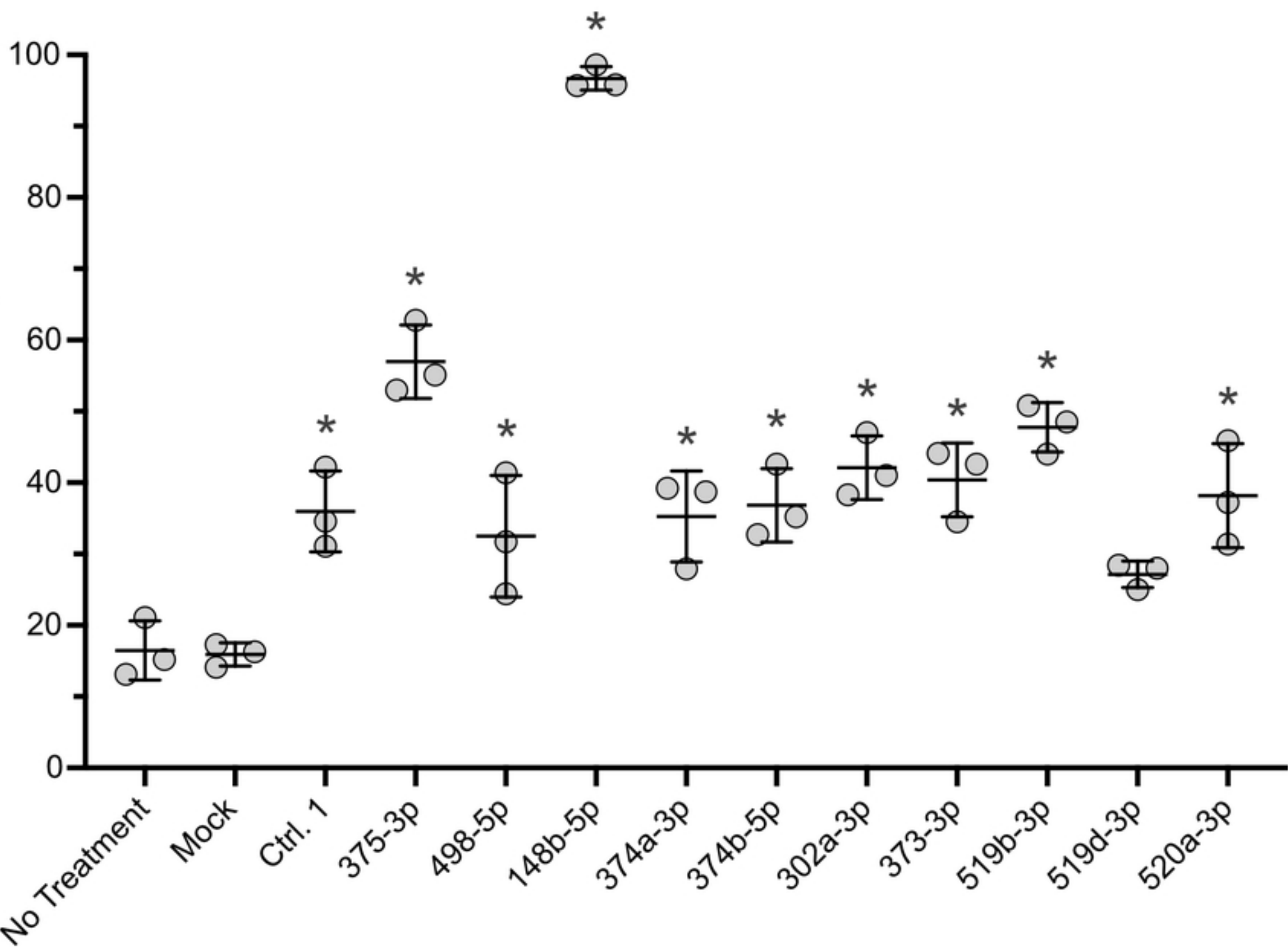


Figure 5



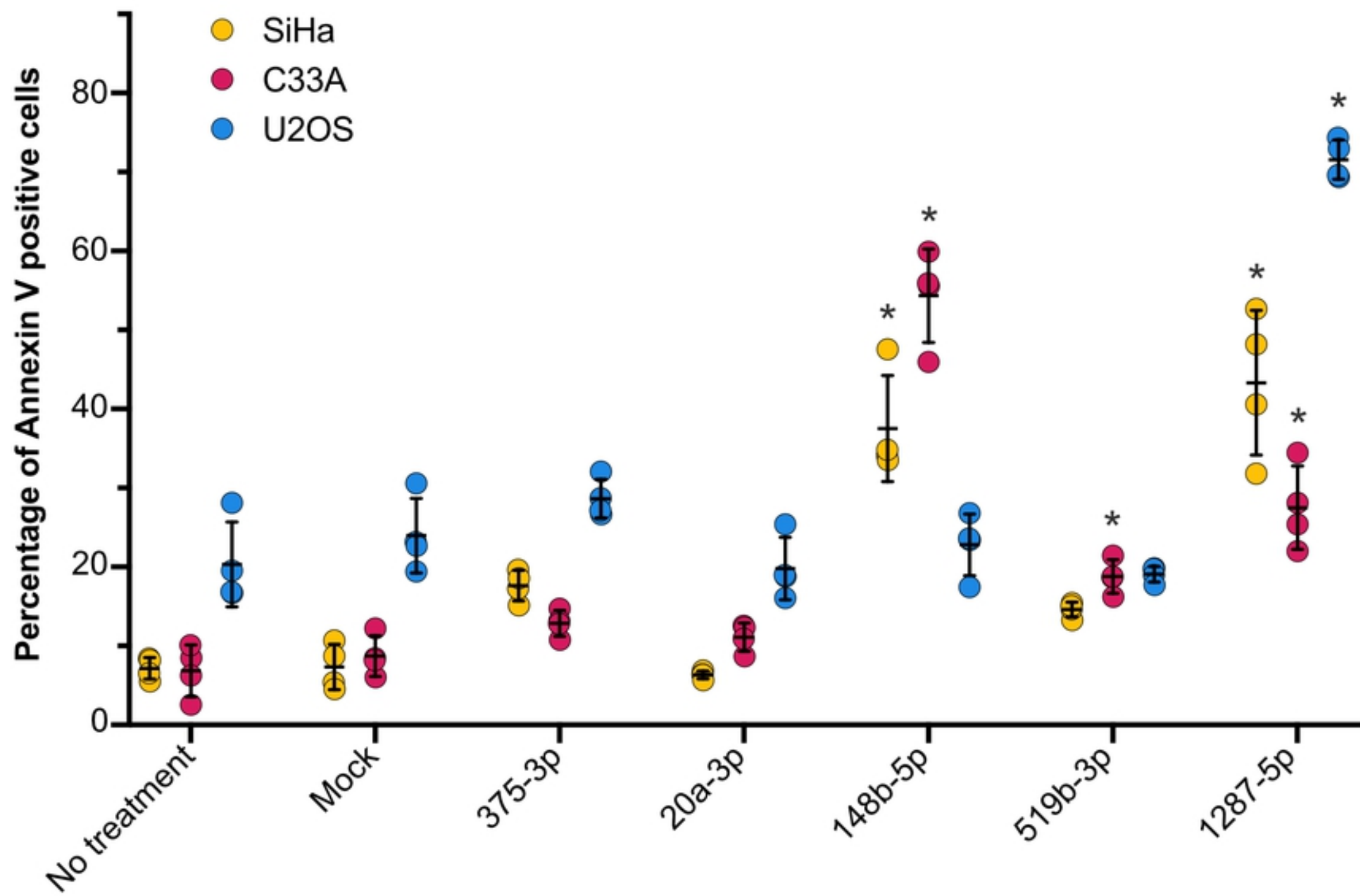


Figure 6

**A.**

bioRxiv preprint doi: <https://doi.org/10.1101/2020.09.21.305946>; this version posted September 21, 2020. The copyright holder for this preprint (which was not certified by peer review) is the author/funder, who has granted bioRxiv a license to display the preprint in perpetuity. It is made available under aCC-BY 4.0 International license.

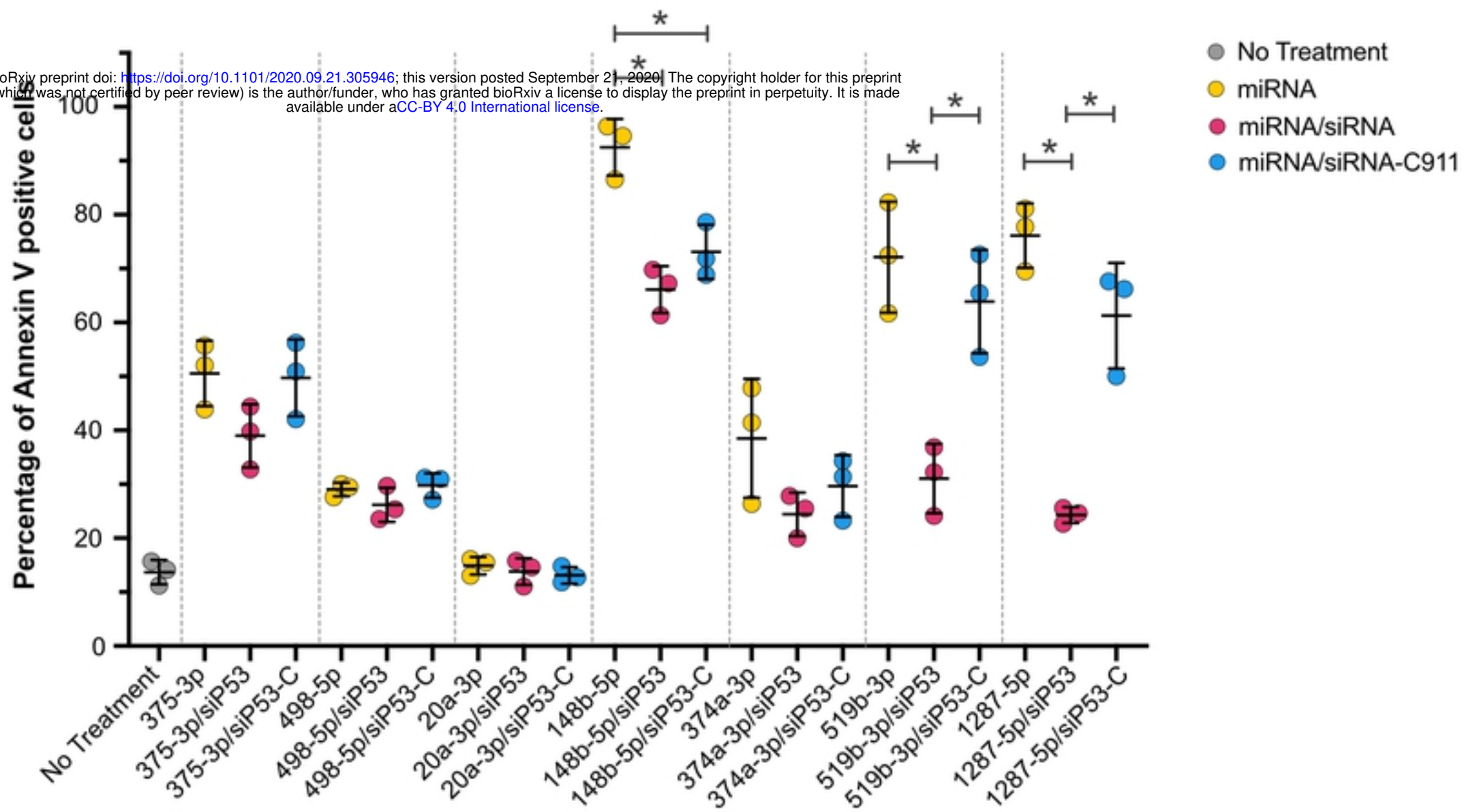
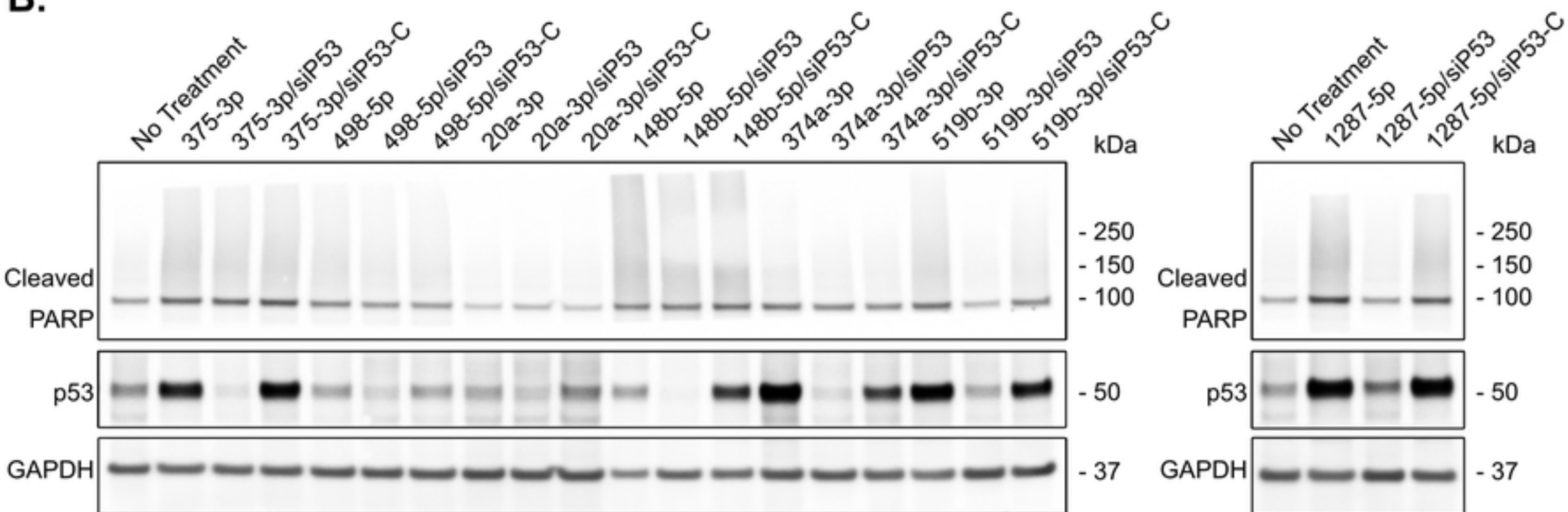
**B.**

Figure 7